July 2016

Chemical Stability of Curcumin: Structure and Activity Relationship (SAR) Study

Zheyuan Du
University of Massachusetts Amherst

Chemical Stability of Curcumin: Structure and Activity Relationship (SAR) Study

A Thesis Presented

by

ZHEYUAN DU

Submitted to the Graduate School of the
University of Massachusetts Amherst in partial
fulfillment of the requirements for the degree of

MASTER OF SCIENCE

May 2016

Food Science

Chemical Stability of Curcumin: Structure and Activity Relationship (SAR) Study

A Thesis Presented

By

ZHEYUAN DU

Approved as to style and content by:

_____

Guodong Zhang, Chair

_____

Hang Xiao, Member

_____

Yeonhwa Park, Member

_____

Eric A. Decker, Department Head

Department of Food Science

ACKNOWLEDGMENTS

I would like to thank my advisor, Guodong Zhang, for his support and patient guidance over the past two years. Thanks are also due to Kailimi Li, Weicang Wang, Julia Zhu, Katherine Z. Sanidad, Elvira Sukamtoh, Yoshiki Nimiya and everyone in Zhang's lab. Their friendship and selfless contribution to my professional development have been invaluable and will forever be appreciated. I would also like to extend my gratitude to the members of my committee, Xiao Hang, Yeonhwa Park, for their helpful comments and suggestions on this project.

I want to thank UMass NMR facilities and Mass Center for their support on my project. I could not achieve so much without their help.

Last but not least, a special thank you to all those whose support and friendship helped me to stay focused on this project and who have provided me with the encouragement to continue when I met with difficulties.

ABSTRACT

CHEMICAL STABILITY OF CURCUMIN: STRUCTURE AND ACTIVITY RELATIONSHIP (SAR) STUDY

MAY 6th 2016

ZHEYUAN DU, B.S., EAST CHINA UNIVERSITY OF SCIENCE AND TECHNOLOGY

M.S., UNIVERSITY OF MASSACHUSETTS AMHERST

Directed by: Professor Guodong Zhang

Over the past decades, numerous studies have shown that curcumin has potent biological activities. As a potential chemopreventing agent, curcumin was demonstrated to exert anti-cancer effects in both in vitro and in vivo studies. However, low bioavailability of curcumin limited human clinical trials and its application to be formulated as therapeutics. In this thesis, we will summarize the anti-cancer effects of curcumin in animal studies and clinical trials. In addition, an SAR study will be introduced to elucidate the mechanism of curcumin degradation at physiological pH. We synthesized various curcumin analogues and compared their stability in phosphate buffer using HPLC and colorimetry assay. The results not only demonstrated that the -OH group and the methoxy group play a critical role in stability of curcumin in physiological environment, but also support the proposed mechanism of phenolic radical formation by which curcumin degrades to its major product bicyclopentadione.

Key words: curcumin, anti-cancer, tumor growth, metastasis, SAR study, physiological pH, phosphate buffer, curcumin analogues, synthesis, bicyclopentadione

TABLE OF CONTENTS

Page

LIST OF TABLES

Table Page

LIST OF FIGURES

Figure Page

CHAPTER 1

LITERATURE REVIEW: ANTI-CANCER EFFECTS OF CURCUMIN

1.1 Introduction

Turmeric, *Curcuma longa* L. rhizomes has been widely used as a spice and to treat abdominal pain, sprain and swelling in both Chinese and Indian medicine [1]. Over the past decades, a number of studies have shown that curcumin, a principal component of turmeric, has potent biological activities such as anti-inflammatory, anti-oxidant and anti-cancer effects [2, 3, 4]. Here in the section below, we will summarize the animal and human studies to evaluate the anti-cancer effects of curcumin.

1.2 Animal studies of curcumin on primary tumor growth

1.2.1 Curcumin inhibits ascites tumor growth

One study in Swiss albino mice showed that after implantation of Ehrlich ascites tumor through subcutaneous injection of DLA cells, i.p. injection of liposomally encapsulated curcumin at a dosage of 50 mg/kg body weight after implantation of Ehrlich ascites tumor (induced by subcutaneous injection of DLA cells), increased the life span of mice by 53.72% and reduced tumor volumes significantly compared to the control group [5].

1.2.2 Curcumin inhibits tumor growth of gastrointestinal cancer

Curcumin was found to inhibit tumor growth induced by colorectal cancer cells (Colo205 cells and LoVo cells) significantly when in female athymic *nu/nu* mice after i.v. injection thrice a week at a dosage of 40 mg/kg body weight [6]. Another group evaluated anti-tumor effect of curcumin on gastric cancer [7]. As a result, curcumin, orally administrated to female athymic

nu/nu mice daily at a dosage of 0-200 mg/kg body weight, was shown to inhibit tumor growth in a dose-dependent manner accompanied with increased life span of mice compared with the control group. This study also indicated a mechanism of inhibiting telomerase activity and inducing apoptosis in cancer cell lines by which curcumin exerted its anti-tumor effect.

1.2.3 Curcumin inhibits tumor growth of brain cancer

One study showed that curcumin could inhibit tumor growth of malignant gliomas by 4-fold on day 16 after adult nude mice was i.t. injected with curcumin at a dosage of 100 mg/kg body weight compared to untreated controls [8]. Treatment of curcumin was found to inhibit the Akt/mammalian target of rapamycin (mTOR)/ p70 ribosomal protein S6 kinase (p70S6K) pathway and activating the extracellular signal-regulated kinases 1/2 (ERK1/2) pathway, the two pathways regulating autophagy. Tumor growth of gliomas in xenograft models was also found to be inhibited by i.p. injection of curcumin at a dosage of 120 mg/kg body weight per day in athymic mice (Crl:CD-1 *nu*BR) leading to significant increase of life span of animals by 12% compared to the control group [9].

1.2.4 Curcumin inhibits tumor growth of head and neck cancer

Curcumin was shown to inhibit tumor growth induced by head and neck squamous cell carcinoma (HNSCC) [10]. In this study, liposomally encapsulated curcumin was i.v. injected to female athymic *nu/nu* mice four times a week for 3.5 weeks at a dosage of 50mg/kg body weight. The result indicated that treatment of curcumin led to the suppression of tumor growth and a reduction of tumor weight by 56.27 mg and 84.43 mg accompanied with the reduction of nuclear expression of NF-κB compared with the groups treated with empty liposomes and untreated controls, respectively.

1.2.5 Curcumin inhibits tumor growth of skin cancer

A study in female B6D2F1 mice demonstrated that curcumin, i.p. injected daily at a dosage of 25 mg/kg body weight combined with treatment of a prophylactic immune preparation of soluble proteins resulted in a slight delay of tumor growth induced by melanoma cells [11]. Additionally, the combination treatment increased survival time by more than 82.8% compared with the group with immune preparation (48.6%) and the group treated with curcumin only (45.7%). Another animal study showed that in female C57BI/6 mice, orally administrated curcumin at a dosage of 1% for 17 days led to a significant reduction of tumor weight compared to the untreated group (0.8 g versus 1.5 g) [12].

1.2.6 Curcumin inhibits tumor growth of ovarian cancer

Tumor growth induced by orthotopic implantation of ovarian cancer cells in female athymic *nu/nu* mice was found to be inhibited by treatment of curcumin only or combination with docetaxel, a commonly used chemotherapy drug [13]. Specifically, for SKOV3ip1 and HeyA8 cell lines respectively, treatment with curcumin which was given by gavage at a dosage of 500 mg/kg body weight led to a 49% and a 55% reduction of tumor growth, while combination treatment resulted in a 96% and a 77% reduction of tumor growth. Additionally, curcumin was shown to exhibit its anti-tumor effect on ovarian cancer through inhibiting Nuclear Factor-κB (NF-κB) activation.

1.2.7 Curcumin inhibits tumor growth of pancreatic cancer

One *in vivo* study indicated that in female athymic *nu/nu* mice, treatment of liposomal curcumin at a dosage of 40 mg/kg body weight (i.v. injection, three times a week for 20 days) resulted in significant inhibition of tumor growth induced by human pancreatic carcinoma cells which was

subcutaneously injected to mice through suppressing NF-κB binding and down-regulating COX-2 and interleukin-8 [14]. Another group evaluated anti-tumor effect of curcumin on pancreas cancer in male athymic *nu/nu* mice [15]. As a result, curcumin given by gavage at a dosage of 1 g/kg body weight per day after one week of tumor implantation significantly enhanced the anti-tumor effect of gemcitabine (i.p. injection, 25 mg/kg twice a week) on pancreatic tumors induced by orthotopic injection through inhibiting NF-κB activation, down-regulating cell proliferation maker Ki-67 and down-regulating microvessel density marker CD31. Specifically, combined treatment of curcumin and gemcitabine resulted in reducing tumor volumes significantly on day 31 of initial treatment compared with controls treated with curcumin only or gemcitabine only.

1.2.8 Curcumin inhibits tumor growth of prostate cancer

Curcumin was also shown to exert anti-tumor effect on prostate cancer in previous studies. In male severe combined immunodeficient (SCID) mice, treatment of curcumin by oral gavage at a dosage of 5 mg/kg body weight three times per week led to significant reduction of mean tumor volumes induced by prostate cancer cells by 4 weeks after tumor inoculation compared to the control group treated with a placebo (168.67 ± 40.7 mm^3 versus 99.57 ± 27.2 mm^3) [16]. Another study showed that in male athymic *nu/nu* mice bearing with tumors induced by a human prostate cell line PC3, tumor growth of PC3 xenografts was inhibited by 50% at 4 weeks after curcumin was given by oral gavage at a dosage of 5 mg/d five times per week by the mechanism of down-regulating MDM2, a cellular ligase of tumor suppressor p53 [17]. In addition, treatment of curcumin was also found to enhance the anti-tumor effect of gemcitabine and radiation in this study. Another *in vivo* study conducted by Dorai te al. [18] indicated that oral administration of curcumin at a dosage of 2% (w/w) in synthetic diets for six weeks resulted in significant decrease

in cell proliferation and increase in the extent of apoptosis accompanied with a significant reduction of microvessel density.

1.2.9 Curcumin inhibits tumor growth of lung cancer

Lev-Ari et al. [19] conducted an animal study to evaluate the anti-tumor effect of curcumin on human non-small cell lung cancer (NSCLC) which has been the leading cause of cancer related mortality. Specifically, curcumin at a dosage of 0.6% in AIN-076 diets was fed to athymic CD-1 nude mice. The effects of curcumin on subcutaneous human NSCLC tumors or orthotopic human NSCLC xenografts were evaluated in ectopic lung tumor mouse models and orthotopic lung tumor mouse models, respectively. Curcumin inhibited subcutaneous tumor growth as seen by a reduction of intra-lung tumor weight by 36% and a significant increase of survival rate through suppressing COX-2 expression. Tumor growth of orthotopic xenografts was also significantly reduced accompanied with increase of survival rate.

1.3 Animal Studies of Curcumin on Chemoprevention

1.3.1 Curcumin prevents gastrointestinal cancer

Curcumin was shown to exhibit anti-tumor activities as a chemopreventive agent in numerous animal studies. Huang et al. [20] investigated inhibitory effects of curcumin on carcinogen-induced tumorigenesis in forestomach, duodenum and colon of mice. The results indicated that treatment of commercial grade curcumin at a dosage of 0.5-2.0% in AIN 76A diet in A/J female mice reduced the numbers of benzo(a)pyrene (B[α]P)-induced forestomach tumor by 51-53% and 47-67% in A/J female mice when administrated during the initiation period and the post-initiation period, respectively. The same dosage of curcumin in AIN 76A diet also resulted in reduction of the numbers of N-ethyl-N'-nitro-N-nitrosoguanidine (ENNG)-induced duodenal

tumors in male C57BL16 mice by 47-77% when administrated during the post-initiation period. In addition, 0.5-4.0% curcumin in AIN 76A diet led to a reduction of the numbers of azoxymethane (AOM)-induced colon tumors by 51-62% when administrated during both the initiation and the post-initiation periods. In another study, male F344 rats were fed with 0.2% and 0.6% curcumin in AIN 76A diet both during the initiation and the post-initiation periods to evaluate the effects on tumorigenesis in colon [21]. When treated at a dosage of 0.2%, curcumin was shown to inhibit the incidence and multiplicity of noninvasive adenocarcinomas by 59% and 71% respectively and the incidence of invasive adenocarcinomas by 54% compared to the mice fed with control diets. Treatment of curcumin at a dosage of 0.6% resulted in a reduction of incidence and multiplicity of noninvasive adenocarcinomas by 78% and 85% respectively and the incidence of invasive adenocarcinomas by 45% compared to the control groups. These results further suggest that curcumin may exhibit its anti-tumor effects on colon cancer in mice in a dose-dependent manner. Curcumin was also shown to inhibit 2-amino-1-methyl-6-phenylimidazo[4,5-b]pyridine (PhIP)-induced tumorigenesis and apoptosis in male *Apc*^{min} mice [22]. Specifically, treatment of curcumin at a dosage of 2000 ppm in diet led to a reduction of the number of tumors in proximal small intestines of mice compared to the mice treated with PhIP alone (2.2 tumors per mouse versus 4.6 tumors per mouse). Shpitz et al. [23] also demonstrated that not only treatment of curcumin alone, but also combination with celecoxib led to inhibition of tumor growth of colorectal cancer in male rats by significantly inhibited the number of aberrant crypt foci (ACF). In another animal study, male F344 rats were fed with 500 ppm curcumin in diet both during initiation and post-initiation periods to evaluate the effects on tumorigenesis of N-nitrosomethylbenzylamine (NMBA)-induced esophageal cancer [24]. Curcumin was shown to inhibit the incidence and multiplicity of esophageal neoplasms by 59%

and 55% respectively compared to the mice fed with control diets during the initiation stage and by 50% and 43% respectively during the post-initiation stage, indicating that curcumin exhibited its chemopreventive effects on NMBA-induced esophageal cancer. Treatment of curcumin at a dosage of 0.05% (w/w) in diet in male Wistar rats was found associated with a reduction of the number of adenocarcinomas of N-methyl-N'-nitro-N-nitrosoguanisine (MNNG)-induced stomach cancer by 66% compared to the group fed with the basal diet [25]. Byun et al. [26] conducted an animal study to evaluate the inhibitory effect of curcumin on AOM-induced colorectal cancer enhanced by high-protein diets (HPD). Specifically, female Balb/c mice were treated with control diets, HPD or HPD containing 0.02% curcumin. As a result, the administration of curcumin led to a significant reduction of tumor multiplicity by 40% compared with the group fed with HPD. Additionally, the expression of COX-2, the levels of nitric oxide and tumor necrosis factor-alpha and the rate of colonocyte proliferation were shown to be significantly inhibited by curcumin, further indicating that curcumin ameliorates the enhancing effect of HPD on colorectal cancer.

1.3.2 Curcumin prevents breast cancer

In female Sprague-Dawley rats, curcumin, i.p. injected at a 100 mg/kg and 200 mg/kg doses, was shown to inhibit 7,12-dimethylbenz[a]anthracene (DMBA)-induced mammary tumorigenesis with a significant reduction of the number of mammary tumors and mammary adenocarcinomas [27]. Another study evaluating the effects of curcumin on preventing mammary tumors showed that in Wistar-MS rats fed with diets containing 1% curcumin, the incidence of diethylstilbestrol (DES)-induced mammary tumors reduced by 28% compared to mice fed with basal diets [28].

1.3.3 Curcumin prevents oral cancer

Curcumin was shown to inhibit the incident of 4-nitroquinoline-1-oxide-induced tongue carcinoma by 91% and oral pre-neoplasia during both initiation and post-initiation stages when orally administrated in dies at a dosage of 0.5 g/kg to male F344 rats [29]. Another study indicated that curcumin at a dosage of 10 mmol/kg in diets or in combination with catechin resulted in a reduction of the number of visible oral papillomas and papilloma volume by 39.6% and 61.3%, respectively in Syrian golden hamsters. Additionally, the incidence of oral squamous cell carcinoma (SCC) and the number of oral SCC lesions was found significantly inhibited by the administration of curcumin [30].

1.3.4 Curcumin prevents liver cancer

In C3H/HeN mice orally treated with diets containing 0.2% curcumin and i.p. injected with N-nitrosodiethylamine (DENA) four days before treatment of curcumin, the multiplicity and hepatocarcinomas were reduced by 81% and 62% after 42 weeks, respectively, compared to the untreated group [31]. The same research group also demonstrated that the treatment of curcumin also resulted in inhibition of hepatic hyperplastic nodules, body weight loss and Curcumin also prevented the induction of hepatic hyperplastic nodules, body weight loss and hypoproteinemia accompanied with increased increased levels of hepatic diagnostic markers in Wistar rats. Curcumin which was i.p. injected to BALB/c mice at a concentration of 200 μM was shown to inhibit liver tumor multiplicity induced by N-bis(2-hydroxypropyl)nitrosamine (DHPN) by 30% [32].

In spite of the potential of curcumin as a chemopreventive agent, other studies have shown that in some animal models, curcumin had no or few chemopreventive effects on certain types of

cancer. Pereira et al. [33] demonstrated that in male Fischer 344 rats, curcumin at 1% and 2% (w/w) doses in diets did not significantly alter the incident and multiplicity of AOM-induced tumors in the colon and DMBA-induced tumors in the mammary gland. The study by Hecht et al. [34] also showed that treatment of curcumin by gavage at the dosage of 2000 ppm in A/J mice had no effect on B[α]P-induced lung tumor multiplicity. Another study in female Sencar mice indicated that 2% curcumin in diets had no effect on the incidence of DMBA-induced tumors, whereas reduced the incidence of leukemias by 53% [35].

1.4 Animal studies of curcumin on metastasis

1.4.1 Curcumin inhibits metastasis of breast cancer

Metastasis plays a critical in spreading of cancer. Therefore, it is of great interest to study the activities of curcumin to inhibit metastatic tumors for potentially being treated as a chemo-therapeutic agent. In male SCID mice, treatment of curcumin by oral gavage at a dosage of 5 mg/kg body weight three times per week was shown to significantly inhibit the number of metastatic pulmonary nodules induced by prostate cancer cells through suppressing the expression of matrix metalloproteinase (MMP)-2, MMP-9 and caspase-3 activity [15]. Another study showed that in female athymic *nu/nu* mice fed with 2% (w/w) curcumin in diets after the primary tumor was surgically removed, the incidence of lung metastasis induced by the human breast cancer xenograft model was significantly reduced through suppressing the expression of NF-κB, COX-2 and MMP-9 indicating the potential of curcumin for chemo-therapeutic application for preventing breast cancer metastasis [36]. The study conducted by Bachmeier et al. [37] focused on anti-metastatic effects of curcumin on breast cancer also indicated that 1% (w/w) curcumin fed to immunodeficient mice resulted in a significant reduction of the incident of lung metastasis by 51% compared to the untreated group through suppressing the expression of

NF-κB and down-regulating of AP-1, further suggesting the potential of curcumin as a chemopreventive agent to prevent metastasis induced by human breast cancer. In another study, dendrosomal curcumin was i.p. injected to BALB/c mice at a dosage of 80 mg/kg body weight to study the inhibitory effect of curcumin on metastasis induced by breast tumor [38]. As a result, treatment of curcumin was shown to be associated with a higher survival rate and a reduction of metastatic signs by 86% compared to the control group in addition to more common metastatic tumors in the lung, the liver and the sternum tissues in the treated groups. Recently, a novel study was conducted to enhance the anti-metastatic effect of curcumin by formulating curcumin with phosphatidylcholine (Meriva) to increase the bioavailability of curcumin [39]. Meriva was shown to inhibit lung metastasis induced by murine mammary gland adenocarcinoma in female athymic nude mice whereas treatment of curcumin alone showed no effect, indicating that this novel conjugated curcumin analog enhance the anti-metastatic activity compared to curcumin.

1.4.2 Curcumin inhibits metastasis of liver cancer

Orally administrated curcumin at a dosage of 100-200 mg/kg body weight for 20 days after the implantation of tumors resulted in significant inhibition of the number of intrahepatic metastasis induced by hepatocellular carcinoma in a dose-dependent manner despite that the growth of tumors was not significantly inhibited by curcumin [40].

1.4.3 Curcumin inhibits metastasis of lung cancer

A study conducted by Chen et al. [41] indicated that p.o. administrated curcumin at a dosage of 1 g/kg body weight for five weeks led to a significant reduction of the number of pulmonary colonized tumor nodules induced by human lung adenocarcinoma cells compared to the control group in SCID mice (3.89 ± 2.28 versus 21.80 ± 13.84 per mouse) through activation of the

tumor suppressor DnaJ-like heat shock protein 40 (HLJ1). Curcumin was also shown to inhibit metastasis induced by orthotopic implantation of Lewis lung carcinoma (LLC-MLN) cell lines in pathogen-free C57BL/6CrSlc mice [42]. Specifically, oral administration of curcumin at 100 or 200 mg/kg doses after implantation of LLC-MLN cells resulted in significant inhibition of the mediastinal lymph node metastasis in a dose-dependent manner in spite of no growth of the tumors at the implantation site. Additionally, administration of curcumin combined with treatment of cis-diamine-dichloroplatinum (CDDP), an anti-cancer drug i.v. injected at a dosage of 7 mg/kg, significantly inhibited the mediastinal lymph node metastasis and tumor growth at the implantation site accompanied with significant prolonged survival time of mice, indicating the enhanced therapeutic effect of curcumin combined with CDDP in terms of inhibiting metastasis.

1.4.4 Curcumin inhibits metastasis of prostate cancer

An animal study of inhibitory effects of curcumin on prostate cancer in Athymic nude mice showed that oral injection of curcumin at a dosage of 30 mg/kg body weight alone or combination with TNF-related apoptosis-inducing ligand (TRAIL) which induces apoptosis of prostate cancer cell lines was associated with anti-metastatic effects *in vivo* including inducing the expression of cell cycle inhibitors p21 and p27 and suppressing the expression of cyclin D1 [43]. Lung metastasis induced by prostate cancer was also found to be inhibited by 1% curcumin in LASCR diets which was fed to CD-1 Foxn1^{nu} male mice [44]. Specifically, treatment of curcumin led to significant inhibition the formation of lung metastases induced by prostate cancer xenografts accompanied with higher number of animals with few metastases by the mechanism of suppressing the expression of proinflammatory cytokines CXCL1 and -2.

1.4.5 Curcumin inhibits metastasis of colorectal cancer

Curcumin, i.v. injected to chicken embryos at the concentration of 12 μM in DMSO, was shown to significantly inhibit distant metastasis induced by Rko cells and HCT116 cells through suppressing the expression of miR-21 which is overexpressed in tumors to promote metastasis, indicating that curcumin exerted its effects on inhibiting metastasis of colorectal cancer cell lines in vivo [45]. Another study also indicated the anti-metastatic effect of curcumin on colorectal cancer in which SCID mice were treated with curcumin by gastric intubation at a dosage of 1 g/kg body weight daily for 30 days [46]. As a result, number of liver metastatic nodules were significantly reduced compared to the control group by the mechanism of suppressing SP-1 regulated genes and focal adhesion kinase (FAK) phosphorylation and up-regulating E-cadherin expression.

1.4.6 Curcumin inhibits metastasis of skin cancer

Menon et al. [47, 48] investigated the inhibitory effects of polyphenolic compounds on lung metastasis induced by B16F10 melanoma cells. The result indicated that oral administration of curcumin at a dosage of 200 nmol/kg body weight in female C57BL/6 mice significantly reduced the number of lung tumor nodules by 80% and increased the life span of mice by 143%, demonstrating the anti-metastatic effects of curcumin on melanoma carcinogen by the mechanism of inhibiting the invasion of B16F10 melanoma cells and inhibiting metalloproteinases

1.5 Clinical studies of curcumin on cancer

1.5.1 Clinical studies of curcumin on colorectal cancer

Curcumin was shown to exert anti-tumor effects in numerous studies indicating that curcumin has the potential to be treated in human as a chemopreventive agent. Many previous and ongoing clinical studies have been conducted to evaluate the anti-tumor activity of curcumin in humans. A clinical study conducted by Sharma et al. [49] recruited patients with colorectal cancer and treated them with curcumin at 36-180 mg doses per day in soft gelatin capsules for 120 days. Among the 15 patients, one patient who exhibited reduced venous blood CEA levels underwent stable disease in the colon but progressive disease in the liver after treated with 36 mg/day curcumin. Five patients exhibited stable disease on CT scan for three months. Furthermore, the stabilization of these five patients was found associated with 59% lower pretreatment lymphocytic glutathione-S-transferase (GST) levels. In another clinical study, among 15 patients with colorectal cancer treated with curcumin at 450-3600 mg doses per day, two patients exhibited stable disease for two months, one of who was stable for four months whereas the other exhibited progressive disease after two months [50]. In addition, LPS-induced PGE2 was found to be lowered by 62% and 57% on day 1 and day 2, respectively, after treatment at the highest dose, indicating that the therapeutic efficacy of curcumin may be related to inducing serum PGE2 levels. A pilot clinical trial conducted by Garcea et al. [51] showed that in 12 patients with hepatic metastasis from colorectal cancer, neither curcumin nor its metabolites was found in the peripheral circulation, whereas trace amount of curcumin metabolites were found in liver tissues after oral administration of curcumin at 450-3600 mg doses per day for 7 days. Difference of oxidative DNA changes was also not significant compared to pretreatment samples. These results suggest that doses of curcumin which can lead to the anti-metastatic

activity may not be applicable in humans currently. Carroll et al. [52] conducted a phase II clinical trial to evaluate the effect of curcumin on colorectal neoplasia. In this study, 44 smokers with eight or more aberrant crypt foci (ACF) were recruited and treated with curcumin at a dosage of 2 g or 4 g per day for 30 days. As a result, for the treatment at 4 g/day, the number of ACF was reduced by 40% whereas no significant reduction was observed for the treatment at 2 g/day. Additionally, five -fold increase in plasma curcumin/conjugate levels was observed at the post-treatment stage suggesting that the resulting reduction of ACF in patients was associated with mediation by curcumin conjugates.

1.5.2 Clinical studies of curcumin on pancreatic cancer

Dhillon et al. [53] conducted a clinical trial to study the effect of curcumin on advanced pancreatic cancer in patients. In this trial, 25 patients with pancreatic cancer were recruited and treated with curcumin at a dosage of 8 g/day for two months. Among these patients, two of them exhibited therapeutic efficacy of curcumin. One patient experienced stable disease for more than 18 months. Tumor regression (73%) was observed in another patient with significant increase of serum cytokine levels by 4 to 35 folds. Additionally, down-regulation of the expression of NF-κB, COX-2 and phosphorylated signal transducer was found associated with the treatment of curcumin in patients. Another clinical study recruiting 21 patients with pancreatic cancer showed that curcumin orally treated at a dosage of 8 g/day in combination with gemcitabine resulted in a median survival time at 161 days and a 1-year survival rate at 19% with no adverse effect triggered by intolerability of curcumin, suggesting that gemcitabine-based chemotherapy of pancreatic cancer can be further investigated [54].

1.5.3 Clinical studies of curcumin on prostate cancer

A recent pilot phase II study showed that after 30 patients with progressing chemotherapy-naive metastatic castration-resistant prostate cancer (CRPC) were administrated with curcumin at a dosage of 6000 mg/day in combination with docetaxel, 59% of the patients were shown prostate-specific antigen (PSA) response and 88% of the responders kept shown PSA response for three cycles of treatment with no adverse effect triggered by curcumin found [55]. These results indicated that randomized clinical trials can be conducted to further evaluate curcumin as a treatment of prostate cancer.

1.5.4 Clinical studies of curcumin on breast cancer

A phase I clinical trial was conducted by Bayet-Robert et al. [56]. In this study, 14 patients with metastatic and advanced breast cancer were recruited. Curcumin was orally administrated at a dosage of 500 mg/day for 7 days and kept administrated at escalated doses until toxicity should occur combined with i.v. injected docetaxel. The results not only indicated a dosage at 8000 mg/day as the maximal dose for toxicity, but also showed some improvements in most patients including decrease of carcinoembryonic antigen and regression of non-measurable lesions without any progressive disease. Additionally, five patients were shown partial responses and three patients experienced stable disease for six weeks after the last cycle of treatment. These results indicated potential of curcumin to be studied as a treatment of metastatic and advanced breast cancer in phase II trials in the future.

1.5.5 Ongoing clinical studies of curcumin on cancer

Although curcumin was shown promising anti-cancer effects in preclinical studies, limited human clinical trials were conducted due to poor bioavailability of curcumin. Many ongoing

clinical trials are making progress on overcoming the knowledge gap and investigating the application of curcumin as a potential chemoreventive agent (www.ClinicalTrials.gov). A study conducted by Baylor Research Institute is ongoing to evaluate the safety and the anti-cancer effect of curcumin combined with FDA-approved chemotherapy drug 5-fluorouracil (5FU, Adracil) on colorectal cancer. Another study sponsored by Emory University is being conducted to investigate the mechanism of curcumin preventing breast cancer through inhibiting NF-kB DNA binding in patients treated by radiotherapy. University of Leicester is conducting a clinical study the chemotherapeutic effects of combination of curcumin and FOLFOX on inhibiting inoperable colorectal metastasis. A study of safety and feasibility of curcumin in preventing Cervical Intraepithelial neoplasias (CIN3) is ongoing in Baylor Research Institute. Centre Jean Perrin has sponsored an ongoing clinical study to investigate the effect of curcumin in combination with Taxotere on treatment of prostate cancer metastatic castration resistant compare to treatment of Taxotere alone.

CHAPTER 2

CHEMICAL STABILITY OF CURCUMIN: STRUCTURE AND ACTIVITY RELATIONSHIP (SAR) STUDY

2.1 Introduction

In spite of potent biological activities of curcumin, the application of curcumin is limited for its poor bioavailability. Wahlstrom et al. [57] found that in Sprague-Dawley rats, when curcumin was orally administrated at a dosage of 1 g/kg, 75% curcumin was excreted from the feces and only trace amount of curcumin was detected in the urine. Another study showed that when curcumin was i.p. and i.v. injected to cannulated rats, most ingested curcumin was excreted in the bile and curcumin was found to be metabolized to glucuronides of tetrahydrocurcumin (THC) and hexahydrocurcumin (HHC) [58]. In a study of Ravindranath et al. [59], curcumin was orally administrated to rats at a dosage of 400 mg/kg. As a result, 40% curcumin was excreted from the feces. In addition, 90% of curcumin was found in the stomach and the small intestine at thirty minutes after administration whereas only 1% was found by 24 hours. One study of Yoshiki et al. [60] indicated that curcumin not only was metabolized in animals, but also degrades rapidly at physiological pH. Furthermore, Griesser et al. [61] demonstrated that bicyclopentadione is the major degradation product of curcumin at physiological pH. Additionally, they proposed a mechanism by which curcumin is transformed to bicyclopentadione through the formation of phenolic radical and cyclic autoxidation (Figure 1). Here in this session, we conducted a research to study the impact of the chemical structure of curcumin on its stability at physiological by synthesizing various curcumin analogues and comparing their stability with curcumin. By doing this research, we will generate a better

understanding of the mechanism of curcumin degradation in physiological environment and thus facilitates the development of curcumin-based therapeutics in the future.

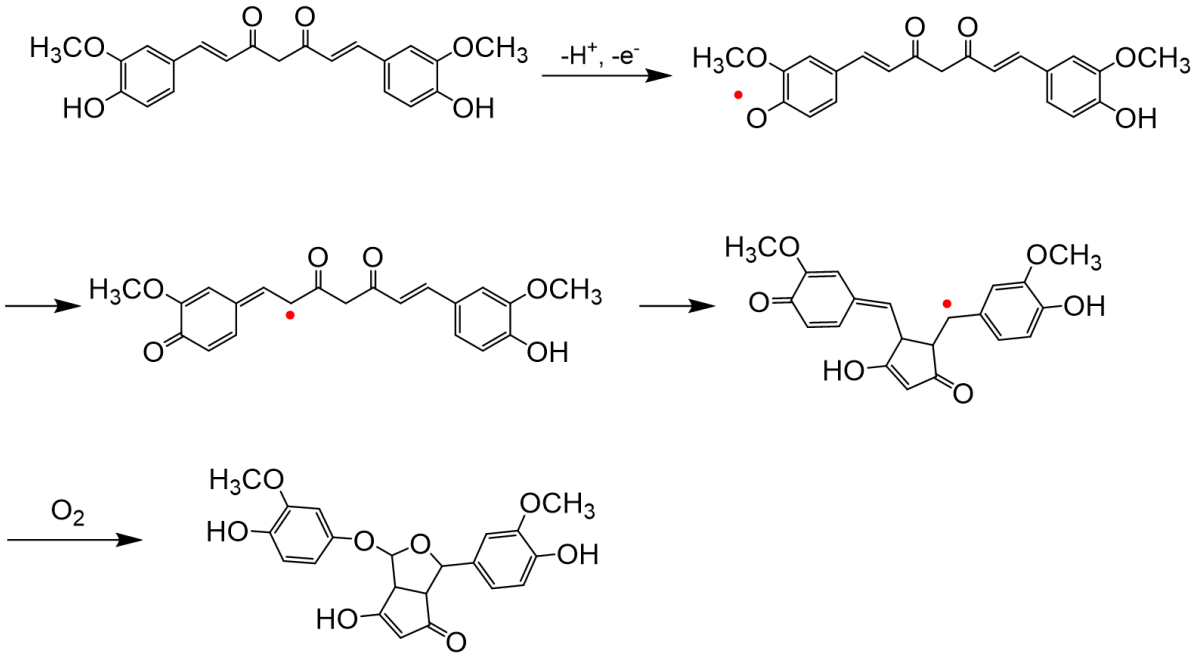

Figure 1. Proposed mechanism of curcumin degradation at physiological pH

2.2 Materials and Methods

2.2.1 Materials

Commercial curcumin, tributyl borate, boron tribromide, propargyl bromide, 4-hydroxybenzalhyde, 3-methyl-4-hydroxybenzalhyde and 3-nitro-4-hydroxybenzalhyde were purchased from Arcos Organics (Waltham, MA, USA). Boric anhydride, acetylacetone, vanillin, 3,4-dimethoxybenzaldehyde, n-butylamine were purchased from Sigma-Aldrich (St. Louis, MO, USA). Magnesium sulfate, sodium phosphate dibasic, potassium phosphate monobasic, potassium carbonate were purchased from Thermal Fisher Scientific (Fair Lawn, MA, USA). 3-bromo-4-hydroxybenzalhyde was purchased from Alfa Aesar, Ward Hill, MA). 3-cloro-4-

hydroxybenzalhyde was purchased from Chem-impex Int'l Inc (Wood Dale, IL, USA). 3-floruo-4-hydroxybenzalhyde was purchased from Oakwood Chemical (N. Estill, SC, USA).
Ethyl acetate, dichloromethane, hexane, HPLC-grade methanol, acetic acid, hydrochloric acid was purchased from Thermal Fisher Scientific. Anhydrous ethyl acetate anhydrous dichloromethane was purchased from Arcos Organics. Tetrahydrofuran was purchased from Sigma-Aldrich. Silica gel for column chromatography was purchased from Natland International Corporation (Morrisville, NC, USA). Silica gel plates for TLC were purchased from EMD Millipore Corporation (Billerica, MA, USA). The rotation evaporator was purchased from Heidolph Brinkmann (Elk Grove Village, IL, USA). Analysis of high resolution ESI-MS was conducted by the Mass Spectrometry Center at UMass Amherst. 'H NMR data were collected on Advance 400 MHz spectrometer from the High-Field NMR Facility at UMass Amherst.

2.2.2 Synthesis of Curcumin

Boric anhydride (0.35 g, 5 mmol) was added to 50 mL anhydrous ethyl acetate, followed by addition of acetylacetone (1.03 mL, 10 mmol). The mixture was stirred at 50℃ for 30 min. Vanillin (3.04 g, 20 mmol) and tributyl borate (10.8 mL, 40 mmol) were added and the mixture was stirred at 50℃ for another 30 min. Then n-butylamine (0.4 mL, 5 mmol) was dissolved in 15 mL anhydrous ethyl acetate and added dropwise. The reaction mixture was stirred under nitrogen at 80℃ for 4 hours and at room temperature overnight. After 30 mL hydrochloric acid was added, the mixture was stirred for 30 min to quench the reaction. The reaction product was extracted with ethyl acetate and the organic layers were combined. The organic layer was washed with water and dehydrated with anhydrous magnesium sulfate. After filtration, the organic layer was dried by the rotation evaporator. The crude product was purified after

recrystallization from methanol. The final product was confirmed by HPLC, high resolution ESI-MS and 'H NMR spectrometry.

2.2.3 Synthesis of Di-*O*-methyl-curcumin

Boric anhydride (0.35 g, 5 mmol) was added to 50 mL anhydrous ethyl acetate, followed by addition of acetylacetone (1.03 mL, 10 mmol). The mixture was stirred at 50℃ for 30 min. 3,4-dimethoxybenzaldehyde (3.32 g, 20 mmol) and tributyl borate (10.8 mL, 40 mmol) were added and the mixture was stirred at 50℃ for another 30 min. Then n-butylamine (0.4 mL, 5 mmol) was dissolved in 15 mL anhydrous ethyl acetate and added dropwise. The reaction mixture was stirred under nitrogen at 80℃ for 4 hours and at room temperature overnight. After 30 mL hydrochloric acid was added, the mixture was stirred for 30min to quench the reaction. The reaction product was extracted with ethyl acetate and the organic layers were combined. The organic layer was washed with water and dehydrated with anhydrous magnesium sulfate. After filtration, the organic layer was dried by the rotation evaporator. The crude product was purified after recrystallization from methanol. The final product was confirmed by HPLC, high resolution ESI-MS and 'H NMR spectrometry.

2.2.4 Synthesis of Di-*O*-demethyl-curcumin

Curcumin (200mg, 0,54mmol) was added to 30 mL anhydrous dichloromethane and the solution was stirred at 0 ℃ for 10 min. Boron tribromide (20 mmol) dissolved in 20 mL anhydrous dichloromethane was then added to the solution dropwise. The reaction mixture was stirred at room temperature overnight. Water was added to the mixture to quench the reaction. The reaction product was extracted with ethyl acetate and the organic layers were combined. The organic layer was washed with water and dehydrated with anhydrous magnesium sulfate. After

filtration, the organic layer was dried with the rotation evaporator. The crude product was purified by column chromatography using 5% methanol in dichloromethane as the mobile phase and silica gel as the stationary phase. The fractions were analyzed by TLC using dichloromethane-methanol-acetate acid (50:5:2) as the eluent mixture. The fractions were then combined and dried by the rotation evaporator. The final product was confirmed by HPLC, high resolution ESI-MS and 'H NMR spectrometry.

2.2.5 Preparation of Curcumin Degradation Products

A solution of curcumin (4.6mg) in tetrahydrofuran (5mL) was added to 1L 0.1 M phosphate buffer (2.59 g/L KH_2PO_4, 11.5 g/L Na_2HPO_4, pH=7.4) to make a 25 μM curcumin solution. The solution was stirred at room temperature for 5 days. The solution was then extracted with equal volume of ethyl acetate. The organic layer was dehydrated with anhydrous magnesium sulfate. After filtration, the organic layer was dried by the rotation evaporator. The dried curcumin degradation products were collected and stored at -20℃.

2.2.6 Isolation of Bicyclopentadione from Curcumin Degradation Products

The curcumin degradation product was dissolved with methanol and analyzed by Agilent 1100 HPLC (Agilent, Santa Clara, CA, USA) using NUCLEOSIL 100-5C18 column (4.6 x 250 mm, 5 μm). The solution was eluted with a multistep gradient of solvent A (water with 0.1% acetic acid) and solvent B (methanol with 0.1% acetic acid) at a flow rate of 1.0 mL/min. The gradient was 20% solvent B increasing to 65% in 15 min, increasing to 90% in 3 min, kept at 90% for 2 min, decreasing to 20% in 2 min and kept at 20% for 3 min. Absorbance at 420 nm was detected to observe the residual curcumin and absorbance at 254 nm was detected to observe the formation of curcumin degradation products in phosphate buffer. Subsequently, the degradation

products in methanol was subjected to Shimadzu-2020 preparative HPLC system (Shimadzu, Marlborough, MA, USA) with the same condition as on Agilent HPLC system. Bicyclopentadione, the major degradation product was isolated by the automatic fraction collector. The fractions were then combined and extracted with ethyl acetate. The organic layer was dehydrated with anhydrous magnesium sulfate. After filtration, the organic layer was dried by the rotation evaporator. The final isolation product was confirmed by HPLC and 'H NMR spectrometry.

2.2.7 Synthesis of Monoalkyne-curcumin

Vanillin (1 g, 6.57 mmol) and potassium carbonate (4.54 g, 33 mmol) were mixed in 50 mL methanol, followed by addition of 80 wt% propargyl bromide solution in toluene (4.91 g, 33 mmol). The reaction mixture was stirred under nitrogen at room temperature overnight. The reaction product was extracted with ethyl acetate and the organic layers were combined. The organic layer was washed with water and dehydrated with anhydrous magnesium sulfate. After filtration, the organic layer was dried by the rotation evaporator. The synthetic alkyne-vanillin was collected and confirmed by HPLC and 'H NMR spectrometry.

Boric anhydride (0.69 g, 10 mmol) was added to 50 mL anhydrous ethyl acetate, followed by addition of acetylacetone (4.12 mL, 40 mmol). The mixture was stirred at 50℃ for 30 min. Subsequently, vanillin (1.52 g, 10 mmol) and tributyl borate (5.38 mL, 20 mmol) were added and the mixture was stirred at 50℃ for another 30 min. Then n-butylamine (0.73 mL, 10 mmol) was dissolved in 15 mL anhydrous ethyl acetate and added dropwise. The reaction mixture was stirred under nitrogen at 80℃ for 4 hours and at room temperature overnight. After 30 mL hydrochloric acid was added, the mixture was stirred for 30 min to quench the reaction. The reaction product was extracted with ethyl acetate and the organic layers were combined. The

organic layer was washed with water and dehydrated with anhydrous magnesium sulfate. After filtration, the organic layer was dried by the rotation evaporator. The crude product was purified by column chromatography using 50% ethyl acetate in hexane as the mobile phase and silica gel as the stationary phase to afford furoylacetone. The fractions were analyzed by TLC using ethyl acetate-hexane (50:50) as the eluent mixture. The fractions were then combined and dried by the rotation evaporator. The purified furoylacetone was then confirmed by HPLC, and 'H NMR spectrometry.

Boric anhydride (0.60 g, 0.85 mmol) was added to 30 mL anhydrous ethyl acetate, followed by addition of furoylacetone (0.40 g, 1.71 mmol). The mixture was stirred at 50℃ for 30 min. Alkyne-vanillin (0.32 g, 1.71 mmol) and tributyl borate (460 µL, 1.71 mmol) were added and the mixture was stirred at 50℃ for another 30 min. Then n-butylamine (169 µL) was dissolved in 10 mL anhydrous ethyl acetate and added dropwise. The reaction mixture was stirred under nitrogen at 80℃ for 4 hours and at room temperature overnight. After 30 mL hydrochloric acid was added, the mixture was stirred for 30 min to quench the reaction. The reaction product was extracted with ethyl acetate and the organic layers were combined. The organic layer was washed with water and dehydrated with anhydrous magnesium sulfate. After filtration, the organic layer was dried by the rotation evaporator. The crude product was purified by column chromatography with an ethyl acetate-hexane gradient from 40:60 to 50:50 to afford monoalkyne-curcumin using silica gel as the stationary phase. The fractions were analyzed by TLC using ethyl acetate-hexane (50:50) as the mobile phase. The fractions were then combined and dried by the rotation evaporator. The purified monoalkyne-curcumin was then confirmed by HPLC, high resolution ESI-MS and 'H NMR spectrometry.

2.2.8 Synthesis of Dialkyne-curcumin

Vanillin (1 g, 6.57 mmol) and potassium carbonate (4.54 g, 33 mmol) were mixed in 50 mL methanol, followed by addition of 80 wt% propargyl bromide solution in toluene (4.91 g, 33 mmol). The reaction mixture was stirred under nitrogen at room temperature overnight. The reaction product was extracted with ethyl acetate and the organic layers were combined. The organic layer was washed with water and dehydrated with anhydrous magnesium sulfate. After filtration, the organic layer was dried by the rotation evaporator. The synthetic alkyne-vanillin was collected and confirmed by HPLC and 'H NMR spectrometry.

Boric anhydride (0.35 g, 5 mmol) was added to 50 mL anhydrous ethyl acetate, followed by addition of acetylacetone (1.03 mL, 10 mmol). The mixture was stirred at 50℃ for 30 min. Alkyne-vanillin (3.8 g, 20 mmol) and tributyl borate (10.8 mL, 40 mmol) were added and the mixture was stirred at 50℃ for another 30 min. Then n-butylamine (0.4 mL, 5 mmol) was dissolved in 15 mL anhydrous ethyl acetate and added dropwise. The reaction mixture was stirred under nitrogen at 80℃ for 4 hours and at room temperature overnight. After 30 mL hydrochloric acid was added, the mixture was stirred for 30 min to quench the reaction. The reaction product was extracted with ethyl acetate and the organic layers were combined. The organic layer was washed with water and dehydrated with anhydrous magnesium sulfate. After filtration, the organic layer was dried by the rotation evaporator. The crude product was purified after recrystallization from methanol. The final product was confirmed by HPLC, high resolution ESI-MS and 'H NMR spectrometry.

2.2.9 Synthesis of 7,7'-R-curcumin

Curcumin analogues 7,7'-R-curcumin (R= H, CH_3, NO_2, Br, Cl, F) were synthesized with the same protocol as curcumin. Briefly, boric anhydride (0.35 g, 5 mmol) was added to 50 mL

anhydrous ethyl acetate, followed by addition of acetylacetone (1.03 mL, 10 mmol). The mixture was stirred at 50℃ for 30 min. 3-R-4-hydroxybenzaldehyde (20 mmol, R= H, CH_3, NO_2, Br, Cl, F) and tributyl borate (10.8 mL, 40 mmol) were added and the mixture was stirred at 50℃ for another 30 min. Then n-butylamine (0.4 mL, 5 mmol) was dissolved in 15 mL anhydrous ethyl acetate and added dropwise. The reaction mixture was stirred under nitrogen at 80℃ for 4 hours and at room temperature overnight. After 30 mL hydrochloric acid was added, the mixture was stirred for 30 min to quench the reaction. The reaction product was extracted with ethyl acetate and the organic layers were combined. The organic layer was washed with water and dehydrated with anhydrous magnesium sulfate. After filtration, the organic layer was dried by the rotation evaporator. The crude products of 7,7'-R-curcumin (R= H, NO_2, Br, Cl, F) were purified after recrystallization from methanol. The 7,7'-dimethyl-curcumin was purified by column chromatography using 35% ethyl acetate in hexane as the mobile phase and silica gel as the stationary phase. The fractions were analyzed by TLC using ethyl acetate-hexane (35:65) as the eluent mixture. The fractions were then combined and dried by the rotation evaporator. The final products were then confirmed by HPLC, and 'H NMR spectrometry.

2.2.10 Stability Assay for Curcumin Analogues

Solutions of curcumin or curcumin analogues at 25 μM were freshly prepared in 0.1 M phosphate buffer (2.59 g/L KH_2PO_4, 11.5 g/L Na_2HPO_4, pH=7.4). The curcumin concentration in the buffer was instantly analyzed at different time points by Agilent 1100 HPLC (Agilent, Santa Clara, CA, USA) using Kromasil 100-5-C18 column (4.6 x 250 mm, 5 μm). The solution was eluted with the mobile phase of 80% methanol with 0.1% acetic acid and 20% water with 0.1% acetic acid at the flow rate of 1.0 mL/min. The detection wavelength was 420 nm.

2.2.11 Colorimetric Assay for Curcumin Analogues

Solutions of curcumin or curcumin analogues at 25 μM were freshly prepared in 0.1 M phosphate buffer (2.59 g/L KH_2PO_4, 11.5 g/L Na_2HPO_4, pH=7.4) and added to a 96-well plate. The absorbance of the solutions at 420 nm was detected at different time points by a plate reader (Molecular Devices, Sunnyvale, CA, USA).

2.3 Results and Discussion

2.3.1 Chemical Synthesis

2.3.1.1 Curcumin

Synthetic curcumin (Figure 2) was obtained as orange powder. Purity of curcumin was checked by Agilent 1100 HPLC (Agilent, Santa Clara, CA, USA) using Kromasil 100-5-C18 column (4.6 x 250 mm, 5 μm) (Figure 3). The compound was eluted with the mobile phase of 80% methanol with 0.1% acetic acid and 20% water with 0.1% acetic acid at the flow rate of 1.0 mL/min. Synthetic curcumin was detected at 420 nm and residual starting material was detected at 254 nm. High resolution ESI-MS showed [M-H^+] at 367.1167. HRMS calcd. for 367.1187. The ^1H NMR showed the signals of the tri-substituted benzene rings at δ 6.92, 7.05, 7.11 ppm. The signals of the methylene group and the methoxy groups were shown at δ 5.85 and 3.95, respectively.

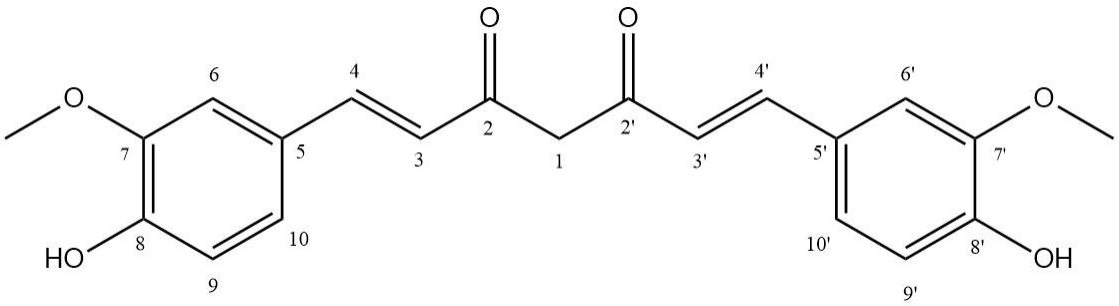

Figure 2. Structure of curcumin

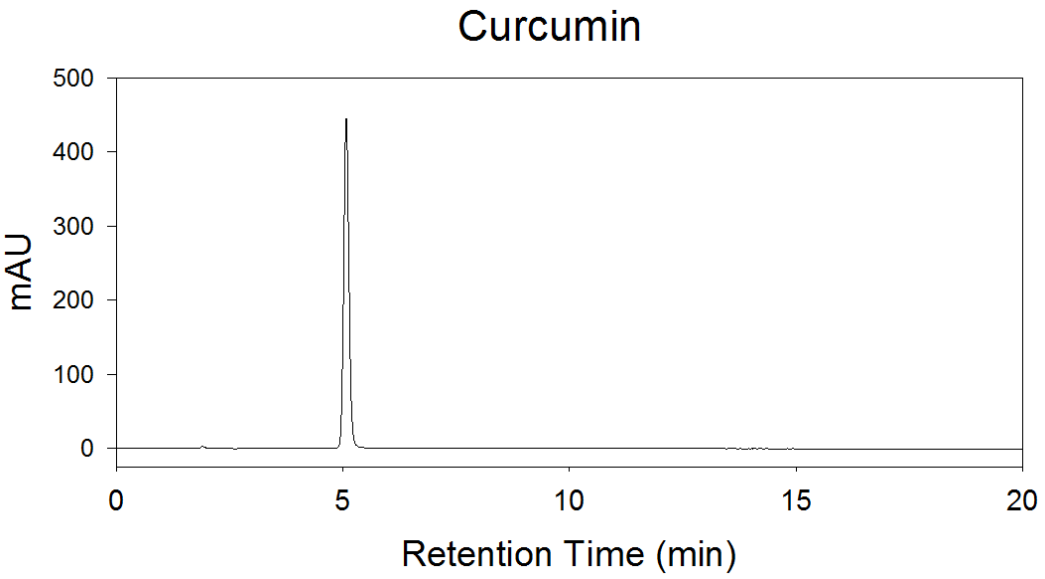

Figure 3. HPLC analysis of curcumin

Table 1. ^{1}H NMR chemical shifts and J-coupling constants for curcumin (400 MHz, chloroform-d) (continued onto next page)

No.	δ ^{1}H (ppm)	Multiplicity	Coupling constant (Hz)
1	5.85	s	—
2	—	—	—
3	6.46	d	15.6

4	7.57	d	15.6
5	—	—	—
6	7.05	d	1.2
7	—	—	—
8	—	—	—
9	6.92	d	8.4
10	7.11	dd	$J_{10\text{-H, }9\text{-H}}$ = 8.4 / $J_{10\text{-H, }6\text{-H}}$ = 2.0
7-OMe	3.95	s	—

2.3.1.2 Di-*O*-methyl-curcumin

Di-*O*-methyl-curcumin (Figure 4) was obtained as orange powder. Purity of the final product was detected by Agilent 1100 HPLC (Agilent, Santa Clara, CA, USA) using Kromasil 100-5-C18 column (4.6 x 250 mm, 5 µm) (Figure 5). The compound was eluted with the mobile phase of 80% methanol with 0.1% acetic acid and 20% water with 0.1% acetic acid at the flow rate of 1.0 mL/min. The synthetic compound was detected at 420 nm and residual starting material was detected at 254 nm. High resolution ESI-MS showed [M-H^+] at 395.1478. HRMS calcd. for 395.1500. The ^{1}H NMR signals of the tri-substituted benzene rings and the methylene group were similar to curcumin. The signals of the methoxy groups at δ 3.93 were shown as a doublet.

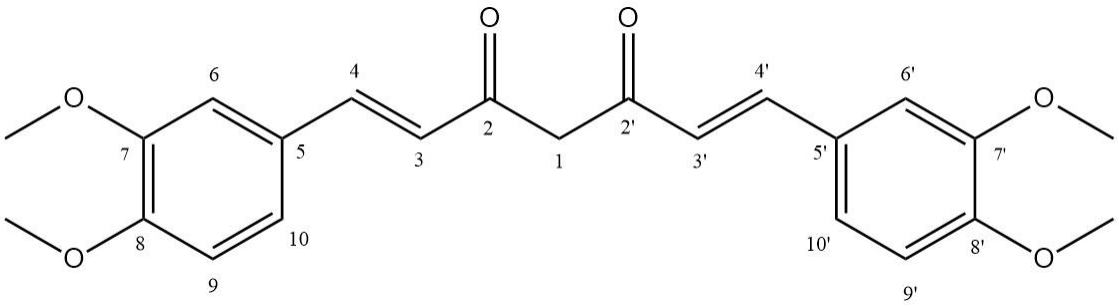

Figure 4. Structure of di-*O*-methyl-curcumin

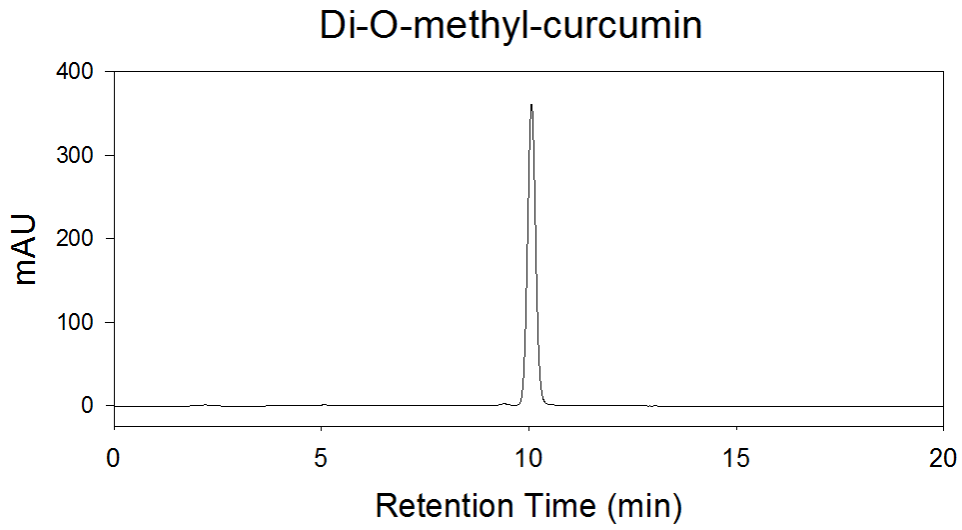

Figure 5. HPLC analysis of di-O-methyl-curcumin

Table 2. ^{1}H NMR chemical shifts and J-coupling constants for di-*O*-methyl-curcumin (400 MHz, chloroform-d) (continued onto next page)

No.	δ ^{1}H (ppm)	Multiplicity	Coupling constant (Hz)
1	5.83	s	—
2	—	—	—

3	6.48	d	16.0
4	7.59	d	16.0
5	—	—	—
6	7.08	d	1.2
7	—	—	—
8	—	—	—
9	6.88	d	8.0
10	7.14	dd	$J_{10\text{-H, }9\text{-H}}$ = 8.0 / $J_{10\text{-H, }6\text{-H}}$ = 1.6
7-OMe, 8-OMe	3.93	d	4.8

2.3.1.3 Di-*O*-demethyl-curcumin

Di-*O*-demethyl-curcumin (Figure 6) was obtained as red plates. Purity of the final product was detected by Agilent 1100 HPLC (Agilent, Santa Clara, CA, USA) using Kromasil 100-5-C18 column (4.6 x 250 mm, 5 µm) (Figure 7). The compound was eluted with the mobile phase of 80% methanol with 0.1% acetic acid and 20% water with 0.1% acetic acid at the flow rate of 1.0 mL/min. The synthetic compound was detected at 420 nm and residual starting material was detected at 254 nm. High resolution ESI-MS showed [M-H^+] at 339.0871. HRMS calcd. for 339.0874. The ^{1}H NMR signals of the tri-substituted benzene rings and the methylene group were similar to curcumin.

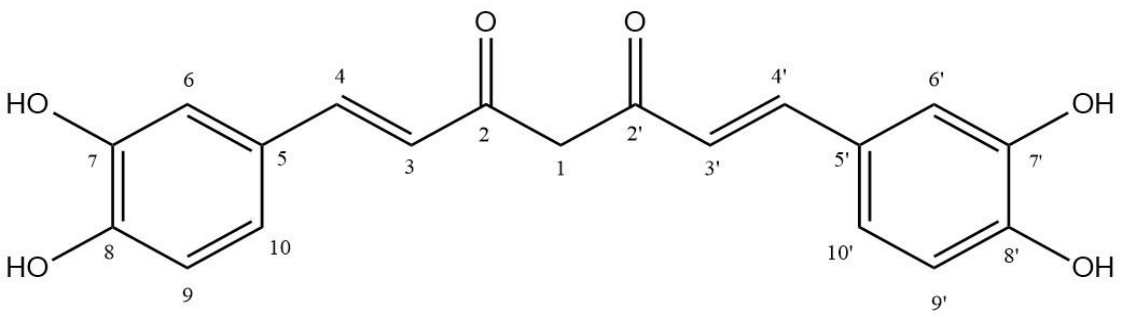

Figure 6. Structure of di-O-demethyl-curcumin

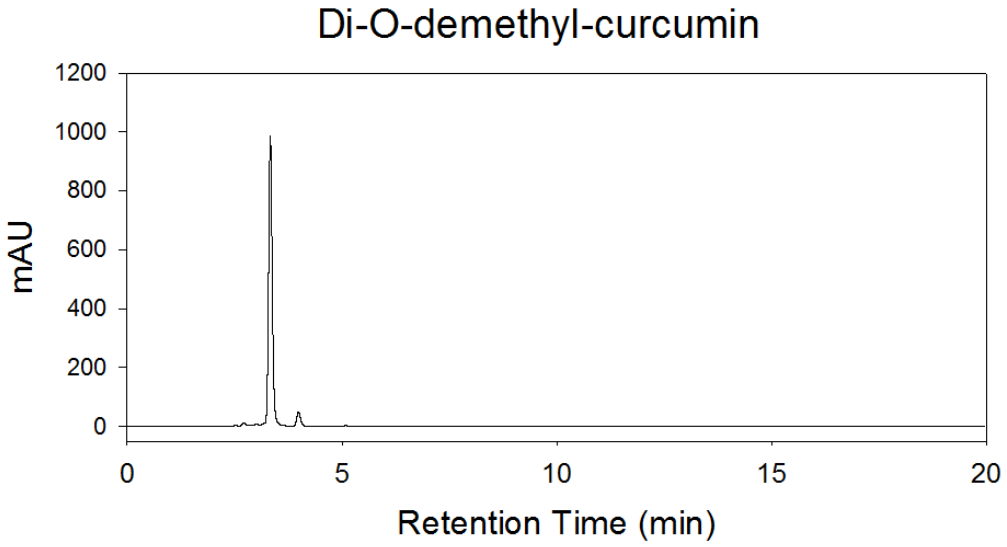

Figure 7. HPLC analysis of di-O-demethyl-curcumin

Table 3. ^{1}H NMR chemical shifts and J-coupling constants for di-*O*-demethyl-curcumin (400 MHz, acetone-d6) (continued onto next page)

No.	δ ^{1}H (ppm)	Multiplicity	Coupling constant (Hz)
1	5.99	s	—
2	—	—	—

3	6.60	d	15.6
4	7.53	d	16.0
5	—	—	—
6	7.20	d	2.0
7	—	—	—
8	—	—	—
9	6.88	d	8.0
10	7.08	dd	$J_{10\text{-H, }9\text{-H}}$ = 8.0 / $J_{10\text{-H, }6\text{-H}}$ = 2.0

2.3.1.4 Monoalkyne-curcumin

Monoalkyne-curcumin (Figure 8) was obtained as orange plates. Purity of the final product was detected by Agilent 1100 HPLC (Agilent, Santa Clara, CA, USA) using Kromasil 100-5-C18 column (4.6 x 250 mm, 5 µm) (Figure 9). The compound was eluted with the mobile phase of 80% methanol with 0.1% acetic acid and 20% water with 0.1% acetic acid at the flow rate of 1.0 mL/min. The synthetic compound was detected at 420 nm and residual starting material was detected at 254 nm. High resolution ESI-MS showed [M-H^+] at 405.1342. HRMS calcd. for 405.1344. The ^{1}H NMR signals of the tri-substituted benzene rings and the methoxy groups were similar to curcumin. The signals of the alkyne group and the methylene group close to the alkyne group were shown at δ 2.53 and 4.80 ppm, respectively.

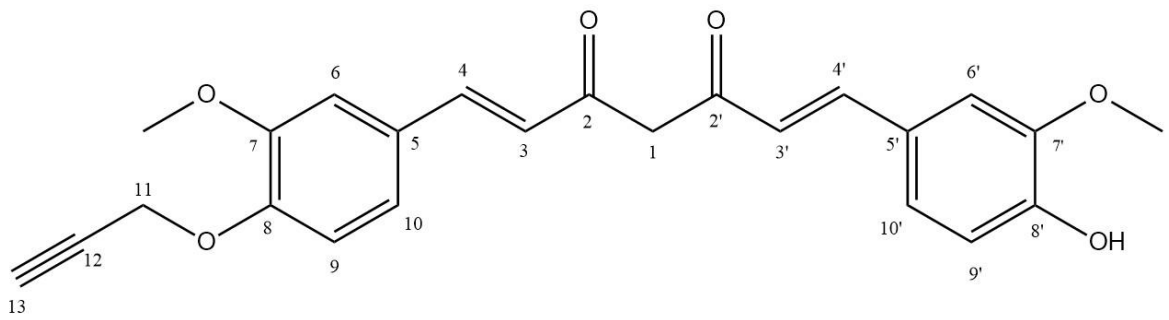

Figure 8. Structure of monoalkyne-curcumin

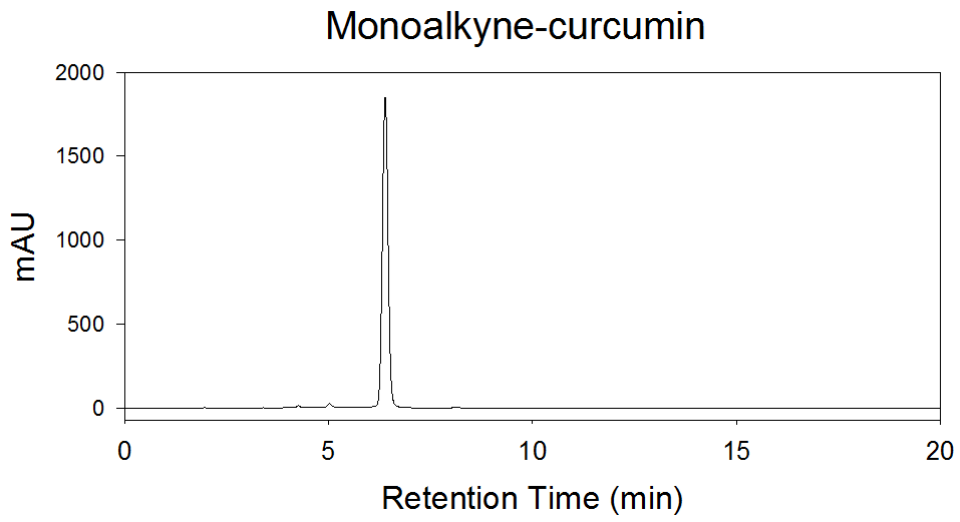

Figure 9. HPLC analysis of monoalkyne-curcumin

Table 4. ^{1}H NMR chemical shifts and J-coupling constants for monoalkyne-curcumin (400 MHz, chloroform-d) (continued across next two pages)

No.	δ ^{1}H (ppm)	Multiplicity	Coupling constant (Hz)
1	5.81	s	—
2	—	—	—
3	6.46	d	16.0

4	7.57	d	15.6
5	—	—	—
6	7.04	d	2.0
7	—	—	—
8	—	—	—
9	6.92	d	8.4
10	7.10	dd	$J_{10\text{-H, }9\text{-H}}$ = 8.0 / $J_{10\text{-H, }6\text{-H}}$ = 2.0
11	4.80	d	2.4
12	—	—	—
13	2.53	t	2.4
7-OMe	3.92	s	—
2’	—	—	—
3’	6.48	d	16.0
4’	7.57	d	15.6
5’	—	—	—
6’	7.08	d	2.0
7’	—	—	—
8’	—	—	—
9’	7.02		7.6
10’	7.12	dd	$J_{10'\text{-H, }9'\text{-H}}$ = 8.4 / $J_{10'\text{-H, }6\text{-H}}$ = 2.0

7’-OMe	3.94	s	—

2.3.1.5 Dialkane-curcumin

Dialkyne-curcumin (Figure 10) was obtained as orange powder. Purity of the final product was detected by Agilent 1100 HPLC (Agilent, Santa Clara, CA, USA) using Kromasil 100-5-C18 column (4.6 x 250 mm, 5 µm) (Figure 11). The compound was eluted with the mobile phase of 80% methanol with 0.1% acetic acid and 20% water with 0.1% acetic acid at the flow rate of 1.0 mL/min. The synthetic compound was detected at 420 nm and residual starting material was detected at 254 nm. High resolution ESI-MS showed [M-H$^+$] at 443.1494. HRMS calcd. for 443.1500. The ^{1}H NMR signals of the tri-substituted benzene rings and the methoxy groups were similar to curcumin. The signals of the alkyne group and the methylene group close to the alkyne group were shown the same as monoalkyne-curcumin.

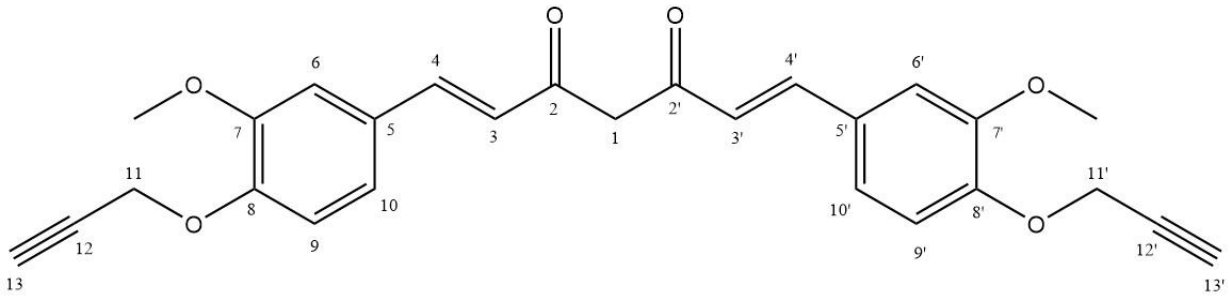

Figure 10. Structure of dialkyne-curcumin

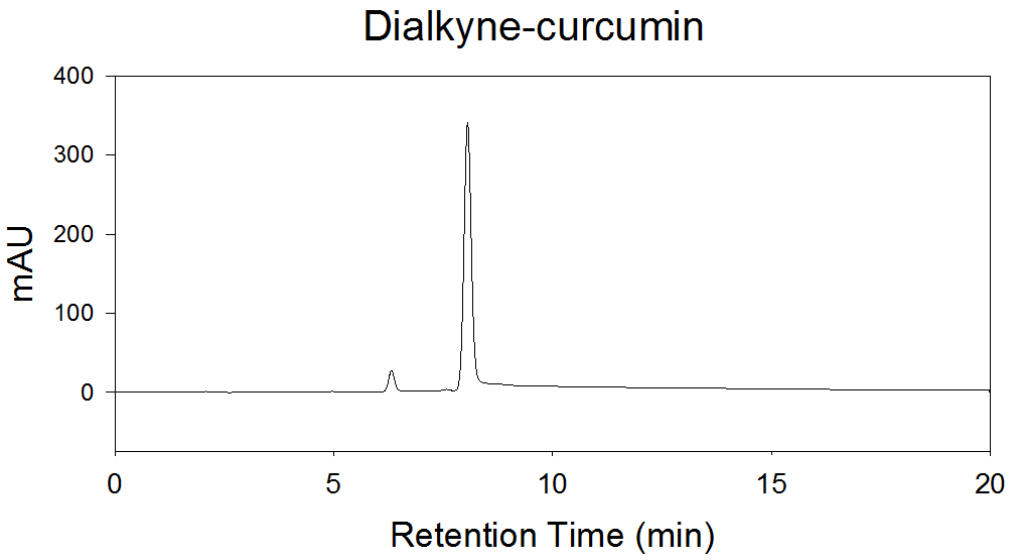

Figure 11. HPLC analysis of dialkyne-curcumin

Table 5. ^{1}H NMR chemical shifts and J-coupling constants for dialkyne-curcumin (400 MHz, chloroform-d) (continued onto next page)

No.	δ ^{1}H (ppm)	Multiplicity	Coupling constant (Hz)
1	5.83	s	—
2	—	—	—
3	6.50	d	16.0
4	7.59	d	16.0
5	—	—	—
6	7.10	d	1.6
7	—	—	—
8	—	—	—

9	7.04	d	8.0
10	7.14	dd	$J_{10\text{-H, }9\text{-H}}$ = 8.4 / $J_{10\text{-H, }6\text{-H}}$ = 1.6
11	4.81	d	2.4
12	—	—	—
13	2.53	t	2.4
7-OMe	3.93	s	—

2.3.1.6 Bisdesmethoxycurcumin

Bisdesmethoxycurcumin (Figure 12) was obtained as red powder. Purity of the final product was detected by Agilent 1100 HPLC (Agilent, Santa Clara, CA, USA) using Kromasil 100-5-C18 column (4.6 x 250 mm, 5 µm) (Figure 13). The compound was eluted with the mobile phase of 80% methanol with 0.1% acetic acid and 20% water with 0.1% acetic acid at the flow rate of 1.0 mL/min. The synthetic compound was detected at 420 nm and residual starting material was detected at 254 nm. High resolution ESI-MS showed $[M+H^+]$ at 309.1140 and $[M+Na^+]$ at 331.0949. HRMS calcd. for $[M+H^+]$ 309.1121 and $[M+Na^+]$ 331.0941. The ^1H NMR signals of the methylene group and the methoxy groups were similar to curcumin. The signals of the bi-substituted benzene rings were shown at δ 6.91 and 7.58 ppm.

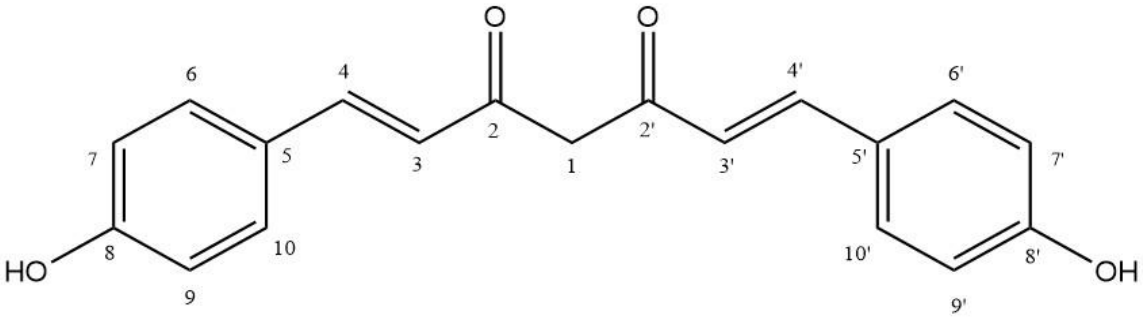

Figure 12. Structure of bisdesmethoxycurcumin

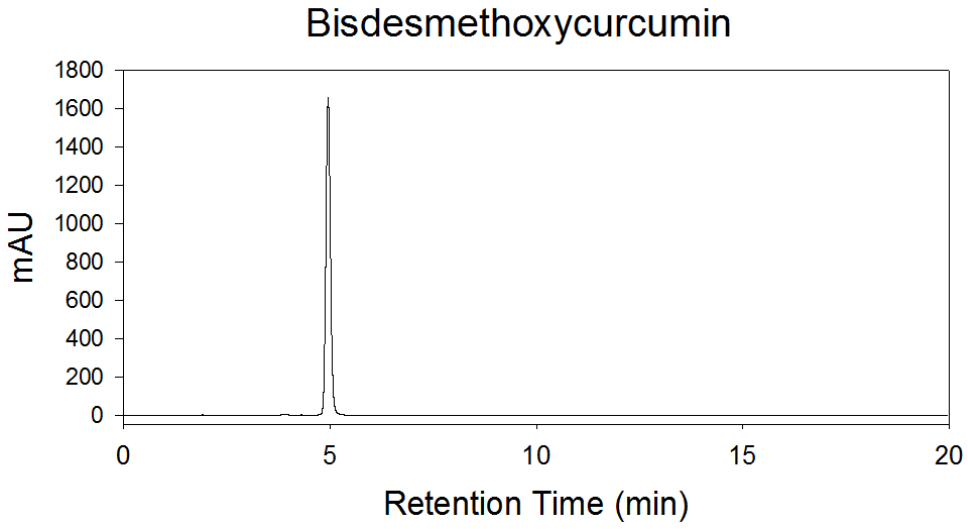

Figure 13. HPLC analysis of bisdesmethoxycurcumin

Table 6. ^{1}H NMR chemical shifts and J-coupling constants for bisdesmethoxycurcumin (400 MHz, chloroform-d) (continued onto next page)

No.	δ ^{1}H (ppm)	Multiplicity	Coupling constant (Hz)
1	6.00	s	—
2	—	—	—
3	6.67	d	16.0

4	7.61	d	16.0
5	—	—	—
6, 10	6.91	d	8.4
7, 9	7.58	d	8.8
8	—	—	—
8-OH	8.90	s	—

2.3.1.7 7,7’-nitro-curcumin

7,7’-nitro-curcumin (Figure 14) was obtained as yellow powder. Purity of the final product was detected by Agilent 1100 HPLC (Agilent, Santa Clara, CA, USA) using Kromasil 100-5-C18 column (4.6 x 250 mm, 5 µm) (Figure 15). The compound was eluted with the mobile phase of 80% methanol with 0.1% acetic acid and 20% water with 0.1% acetic acid at the flow rate of 1.0 mL/min. The synthetic compound was detected at 420 nm and residual starting material was detected at 254 nm. High resolution ESI-MS showed [M-H^+] at 397.0685. HRMS calcd. for 397.0666. The ^{1}H NMR signals of the tri-substituted benzene rings and the methylene group were similar to curcumin.

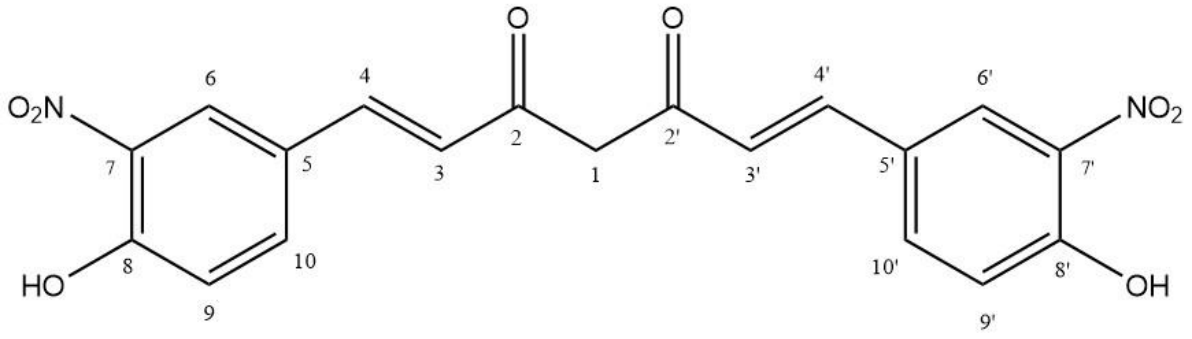

Figure 14. Structure of 7,7’-nitro-curcumin

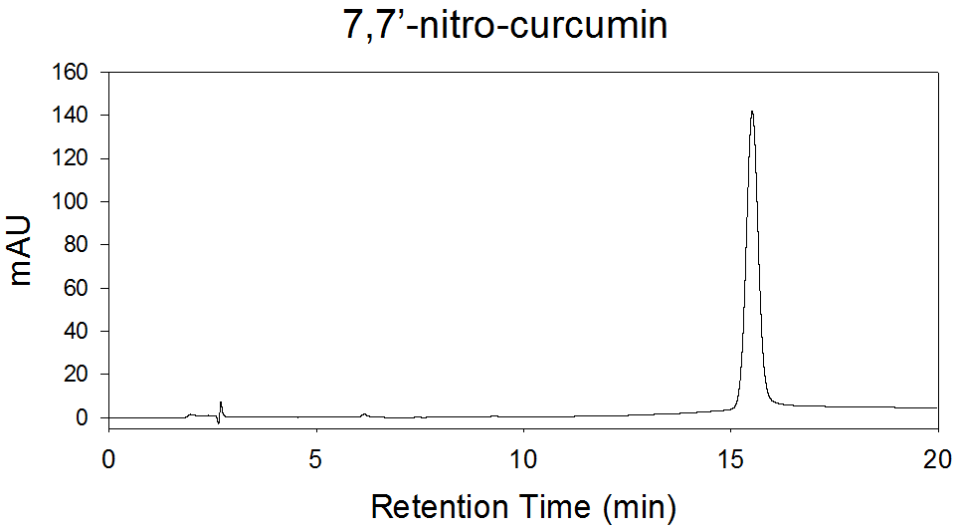

Figure 15. HPLC analysis of 7,7’-nitro-curcumin

Table 7. ^{1}H NMR chemical shifts and J-coupling constants for 7,7’-nitro-curcumin (400 MHz, acetone-d6) (continued onto next page)

No.	δ ^{1}H (ppm)	Multiplicity	Coupling constant (Hz)
1	6.17	s	—
2	—	—	—
3	6.93	d	16.0
4	7.71	d	16.0
5	—	—	—
6	8.44	d	2.0
7	—	—	—
8	—	—	—

9	7.28	d	8.8
10	8.07	dd	$J_{10\text{-H, }9\text{-H}}$ = 8.8 / $J_{10\text{-H, }6\text{-H}}$ = 2.0

2.3.8 7,7’-methyl-curcumin

7,7’-methyl-curcumin (Figure 16) was obtained as orange plates. Purity of the final product was detected by Agilent 1100 HPLC (Agilent, Santa Clara, CA, USA) using Kromasil 100-5-C18 column (4.6 x 250 mm, 5 µm) (Figure 17). The compound was eluted with the mobile phase of 80% methanol with 0.1% acetic acid and 20% water with 0.1% acetic acid at the flow rate of 1.0 mL/min. The synthetic compound was detected at 420 nm and residual starting material was detected at 254 nm. High resolution ESI-MS showed [M+H$^+$] at 337.1429 and [M+Na$^+$] at 359.1243. HRMS calcd. for [M+H$^+$] 337.1434 and [M+Na$^+$] 359.1254. The ^{1}H NMR signals of the tri-substituted benzene rings, the methylene group and the methoxy groups were similar to curcumin. The signal of the methyl groups was shown at δ 2.25 ppm.

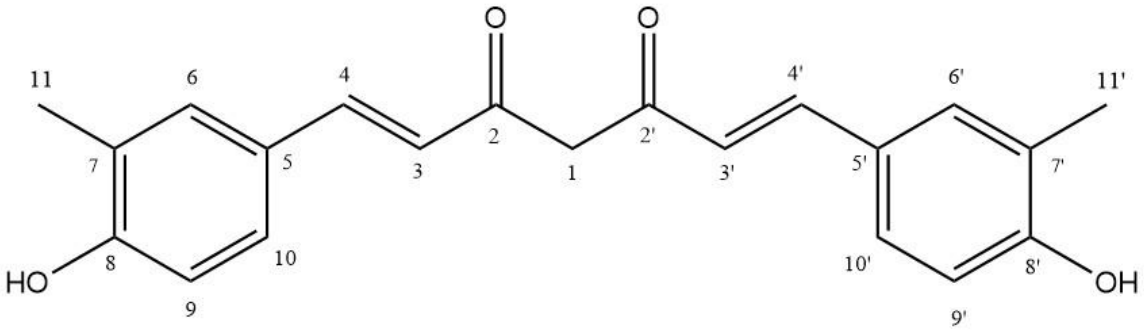

Figure 16. Structure of 7,7’-methyl-curcumin

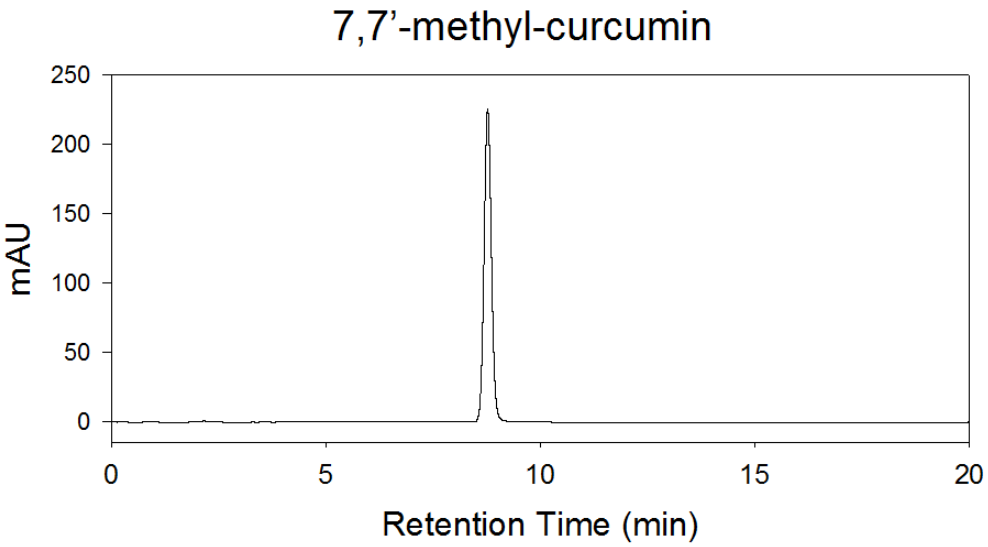

Figure 17. HPLC analysis of 7,7'-methyl-curcumin

Table 8. ^{1}H NMR chemical shifts and J-coupling constants for 7,7'-methyl-curcumin (400 MHz, acetone-d6) (continued onto next page)

No.	δ ^{1}H (ppm)	Multiplicity	Coupling constant (Hz)
1	5.99	s	—
2	—	—	—
3	6.65	d	15.6
4	7.57	d	16.0
5	—	—	—
6	7.50	d	2.0
7	—	—	—
8	—	—	—
9	6.89	d	8.0

10	7.38	dd	$J_{10\text{-H, }9\text{-H}}$ = 8.4 / $J_{10\text{-H, }6\text{-H}}$ = 2.0
11	2.25	s	—

2.3.1.9 7,7’-bromo-curcumin

7,7’-bromo-curcumin (Figure 18) was obtained as yellow powder. Purity of the final product was detected by Agilent 1100 HPLC (Agilent, Santa Clara, CA, USA) using Kromasil 100-5-C18 column (4.6 x 250 mm, 5 µm) (Figure 19). The compound was eluted with the mobile phase of 80% methanol with 0.1% acetic acid and 20% water with 0.1% acetic acid at the flow rate of 1.0 mL/min. The synthetic compound was detected at 420 nm and residual starting material was detected at 254 nm. High resolution ESI-MS showed [M-H^+] at 462.9180, 464.9162 and 466.9147. HRMS calcd. for 462.9286, 464.9167 and 466.9150. The ^{1}H NMR signals of the tri-substituted benzene rings and the methylene group were similar to curcumin.

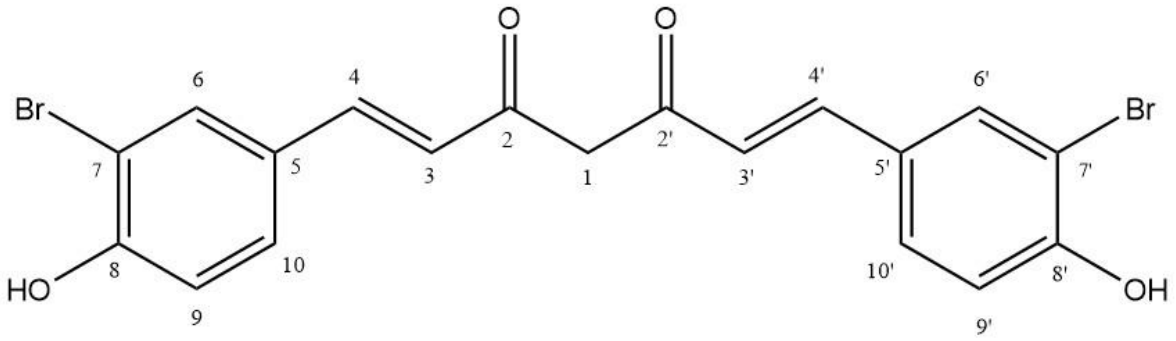

Figure 18. Structure of 7,7’-bromo-curcumin

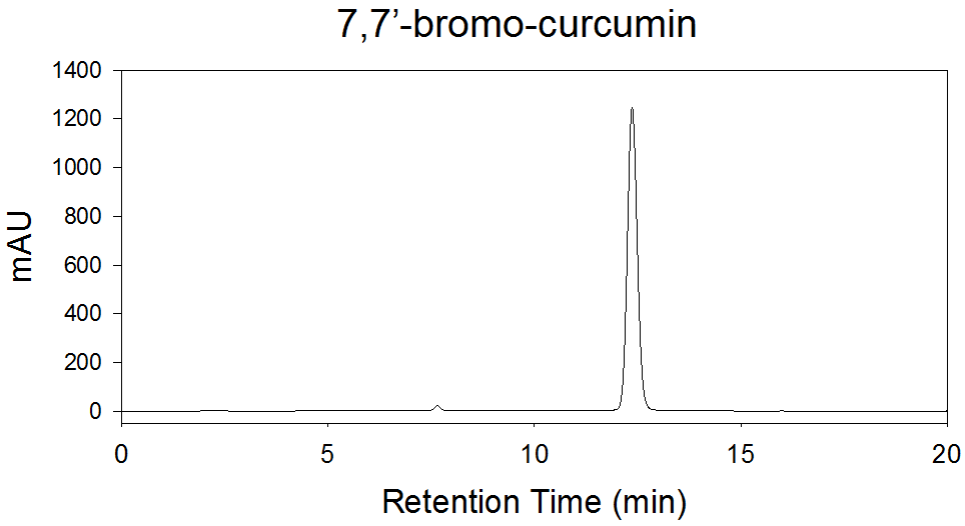

Figure 19. HPLC analysis of 7,7'-bromo-curcumin

Table 9. ^{1}H NMR chemical shifts and J-coupling constants for 7,7'-bromo-curcumin (400 MHz, acetone-d6) (continued onto next page)

No.	δ ^{1}H (ppm)	Multiplicity	Coupling constant (Hz)
1	6.05	s	—
2	—	—	—
3	6.76	d	16.0
4	7.57	d	16.4
5	—	—	—
6	7.92	d	2.0
7	—	—	—
8	—	—	—
9	7.07	d	8.4

10	7.57	dd	$J_{10\text{-H, }9\text{-H}} = 8.4$ / $J_{10\text{-H, }6\text{-H}} = 2.0$

2.3.1.10 7,7’-chloro-curcumin

7,7’-cloro-curcumin (Figure 20) was obtained as yellow powder. Purity of the final product was detected by Agilent 1100 HPLC (Agilent, Santa Clara, CA, USA) using Kromasil 100-5-C18 column (4.6 x 250 mm, 5 µm) (Figure 21). The compound was eluted with the mobile phase of 80% methanol with 0.1% acetic acid and 20% water with 0.1% acetic acid at the flow rate of 1.0 mL/min. The synthetic compound was detected at 420 nm and residual starting material was detected at 254 nm. High resolution ESI-MS showed [M-H$^+$] at 375.0191 and 377.0168. HRMS calcd. for 375.0196 and 377.0171. The ^{1}H NMR signals of the tri-substituted benzene rings and the methylene group were similar to curcumin.

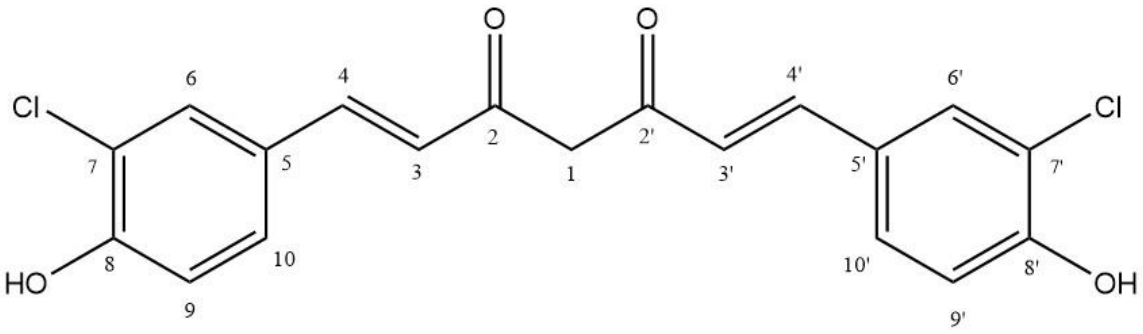

Figure 20. Structure of 7,7’-chloro-curcumin

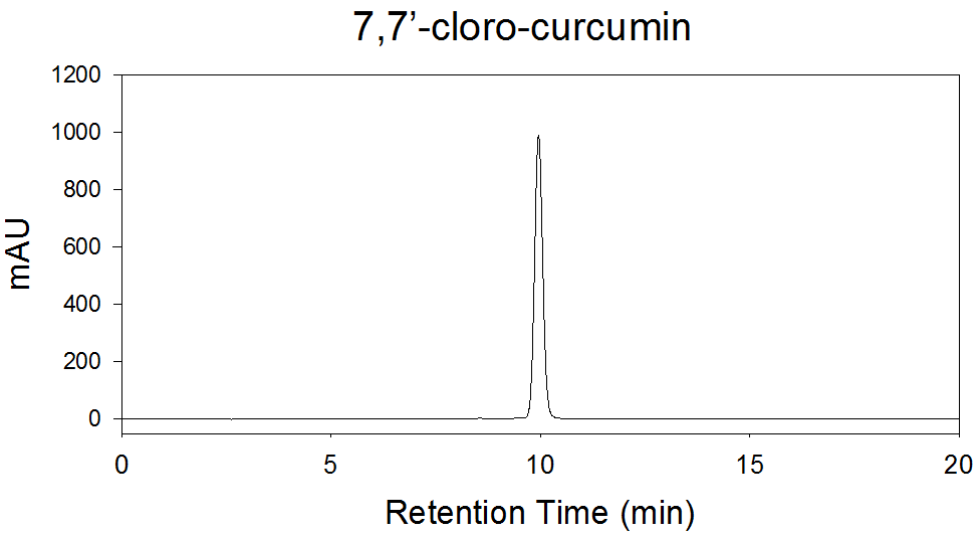

Figure 21. HPLC analysis of 7,7'-chloro-curcumin

Table 10. ^{1}H NMR chemical shifts and J-coupling constants for 7,7'-chloro-curcumin (400 MHz, acetone-d6) (continued onto next page)

No.	δ ^{1}H (ppm)	Multiplicity	Coupling constant (Hz)
1	6.05	s	—
2	—	—	—
3	6.77	d	15.6
4	7.58	d	15.6
5	—	—	—
6	7.76	d	2.0
7	—	—	—
8	—	—	—
9	7.08	d	8.4

10	7.53	dd	$J_{10\text{-H, }9\text{-H}}$ = 8.4 / $J_{10\text{-H, }6\text{-H}}$ = 2.0

2.3.1.11 7,7’-flouro-curcumin

7,7’-floruo-curcumin (Figure 22) was obtained as yellow powder. Purity of the final product was detected by Agilent 1100 HPLC (Agilent, Santa Clara, CA, USA) using Kromasil 100-5-C18 column (4.6 x 250 mm, 5 µm) (Figure 23). The compound was eluted with the mobile phase of 80% methanol with 0.1% acetic acid and 20% water with 0.1% acetic acid at the flow rate of 1.0 mL/min. The synthetic compound was detected at 420 nm and residual starting material was detected at 254 nm. High resolution ESI-MS showed [M-H$^+$] at 343.0789. HRMS calcd. for 343.0787. The ^{1}H NMR signals of the methylene group were similar to curcumin. The signals of the tri-substituted benzene rings were shown as s triplet at δ 7.05 ppm and doubling doublets at 7.52 ppm.

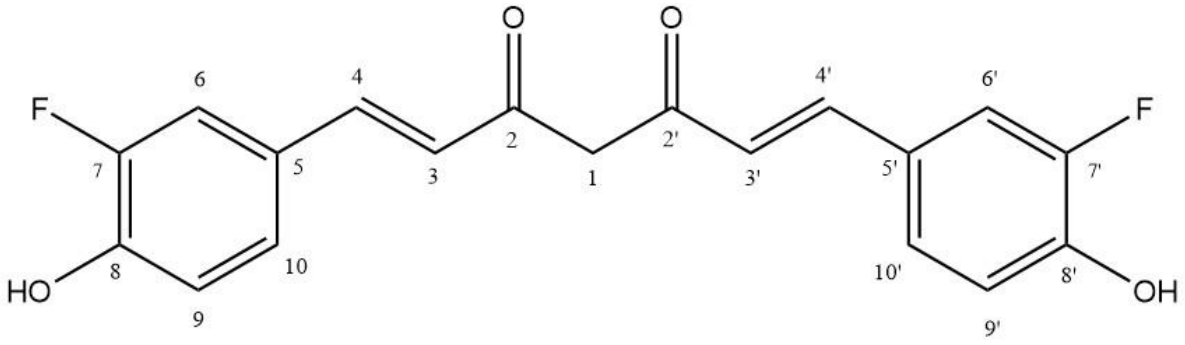

Figure 22. Structure of 7,7’-fluoro-curcumin

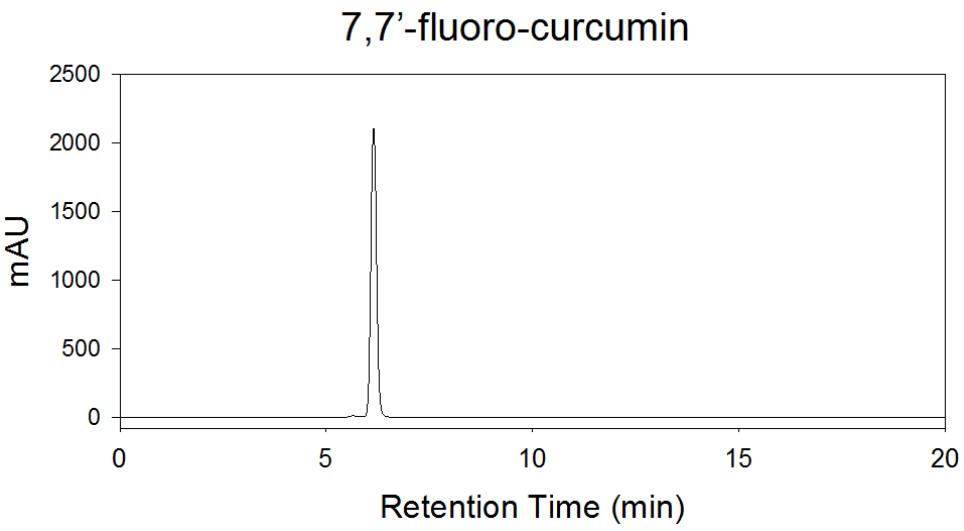

Figure 23. HPLC analysis of 7,7'- fluoro -curcumin

Table 11. ^{1}H NMR chemical shifts and J-coupling constants for 7,7'-fluoro-curcumin (400 MHz, acetone-d6) (continued onto next page)

No.	δ ^{1}H (ppm)	Multiplicity	Coupling constant (Hz)
1	6.03	s	—
2	—	—	—
3	6.74	d	15.6
4	7.58	d	16.0
5	—	—	—
6	7.52	dd	12.4 / 2.0
7	—	—	—
8	—	—	—
9	7.05	t	8.4

10	7.38	dd	$J_{10\text{-H, }9\text{-H}}$ = 8.4 / $J_{10\text{-H, }6\text{-H}}$ = 2.0

2.3.2 Isolation of Bicyclopentadione from Curcumin Degradation Products

Bicyclopentadione was obtained from curcumin degradation products. Purity of the final product was analyzed with HPLC as described in 3.2.6. With confirmation of ^{1}H NMR data (Table 12), we demonstrated that as reported in previous studies, bicyclopentadione is the major product of curcumin degradation in phosphate buffer at pH=7.

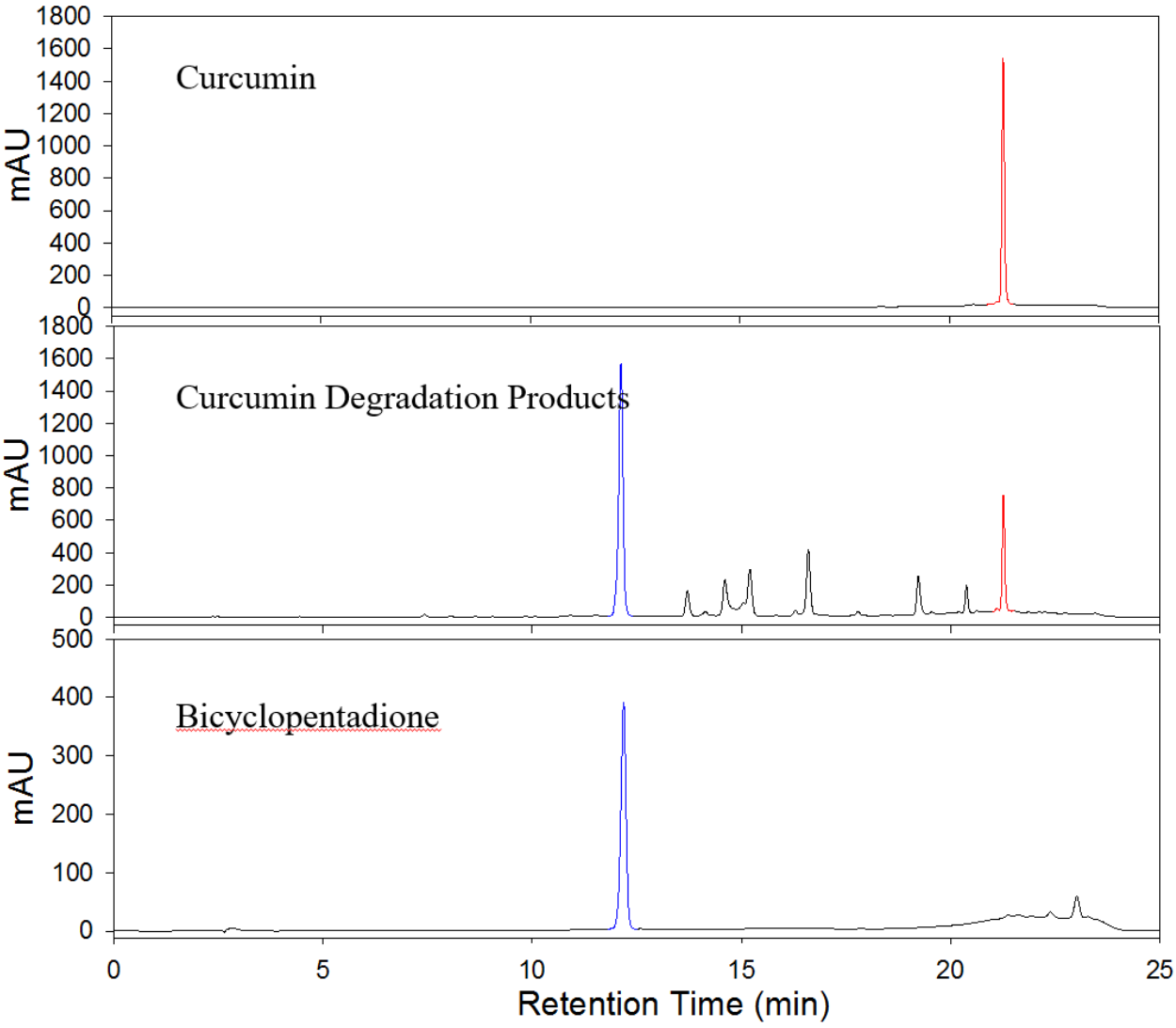

Figure 24. HPLC analysis of curcumin degradation products and bicyclepentadione

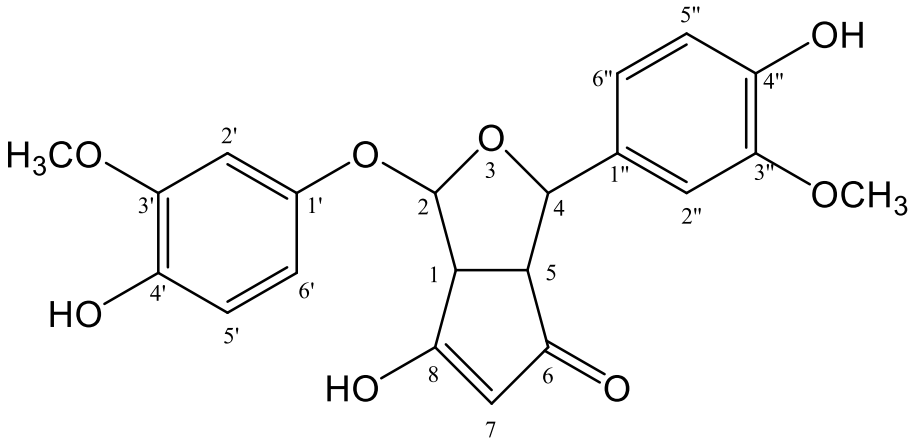

Figure 25. Structure of bicyclopentadione

Table 12. ^{1}H NMR chemical shifts and J-coupling constants for bicyclopentadione (400 MHz, acetone-d6) (continued onto next page)

No.	δ ^{1}H (ppm)	Multiplicity	Coupling constant (Hz)
1	3.63	d	6.0
2	5.90	s	—
4	5.41	d	8.0
5	3.26	d	6.0
6	—	—	—
7	4.89	d	1.0
8	—	—	—
1’	—	—	—
2’	6.92	d	2.4
3’	—	—	—
4’	—	—	—
5’	6.88	d	8.4
6’	6.70	d	2.4
3’-OMe	3.88	s	—
1’’	—	—	—
2’’	6.84	d	1.2
3’’	—	—	—

4''	—	—	—
5''	6.68	d	8.4
6''	6.73	dd	2.0 / 8.0
3''-OMe	3.76	s	—

2.3.3 Stability of Curcumin Analogues Analyzed with HPLC

The HPLC analysis showed that in 120 minutes, di-*O*-methyl-curcumin is much more stable than curcumin in phosphate buffer (Figure 26). This result indicates that the -OH group plays a critical role in curcumin stability at physiological pH. It further supports the proposed mechanism of curcumin's autoxidation by forming phenolic radicals because we synthesized di-*O*-methyl-curcumin to block the -OH group by replacing it with the methoxy group. Additionally, the HPLC analysis also shows that curcumin analogues with different R groups also exhibited different stability in phosphate buffer which means the methoxy group also contributes to curcumin stability at physiological pH (Figure 27). Specifically, the stability of curcumin analogues was in the order of $-NO_2$ > -H > $-OCH_3$. The $-OCH_3$ is an *ortho*- and *para*-directing activator, which means they can decrease the bond dissociation energy (BDE) to form phenolic radicals. On the contrary, the $-NO_2$ group is an *ortho*- and *para*- directing activator which increased the BDE to form phenolic radicals. This result also supports the proposed mechanism of curcumin autoxidation.

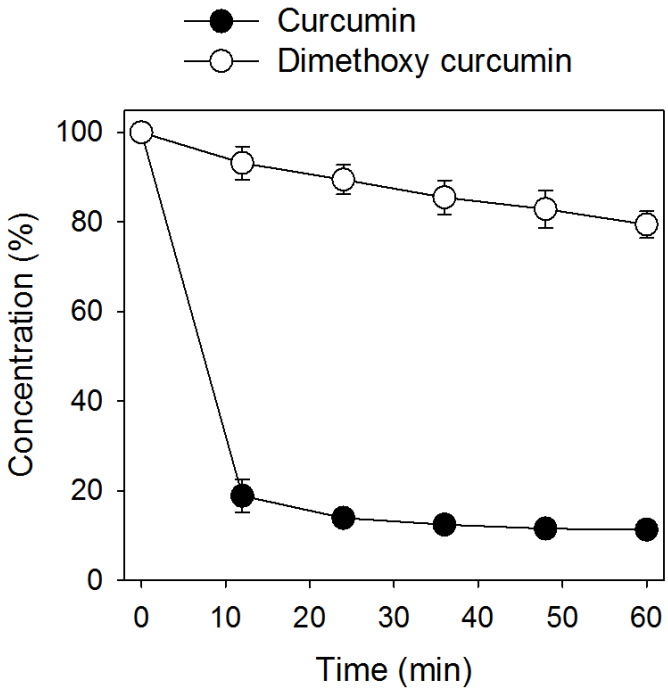

Figure 26. Stability of curcumin and di-O-methyl-curcumin analyzed with HPLC

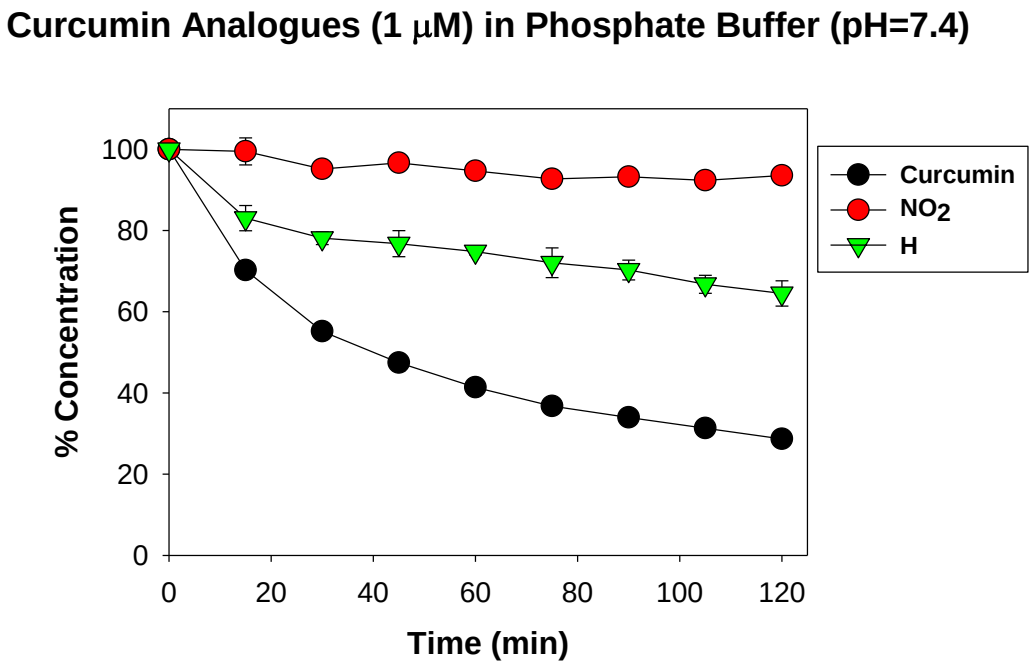

Figure 27. Stability of 7,7'-R-curcumin analyzed with HPLC

2.3.4 Stability of Curcumin Analogues Analyzed with Colorimetry Assay

The colorimetry assay showed that the order stability of curcumin analogues was: -NO_2 > -Br, -Cl > -OCH_3, -CH_3 (Figure 28). Among these groups, -NO_2, -Br and -Cl are *ortho*- and *para*-directing deactivators whereas -OCH_3 and -CH_3 are *ortho*- and *para*- directing activators. This result was consistent with that of HPLC analysis, further supporting the mechanism of phenolic radical formation by which curcumin degrades at physiological pH and forms bicyclopentadione.

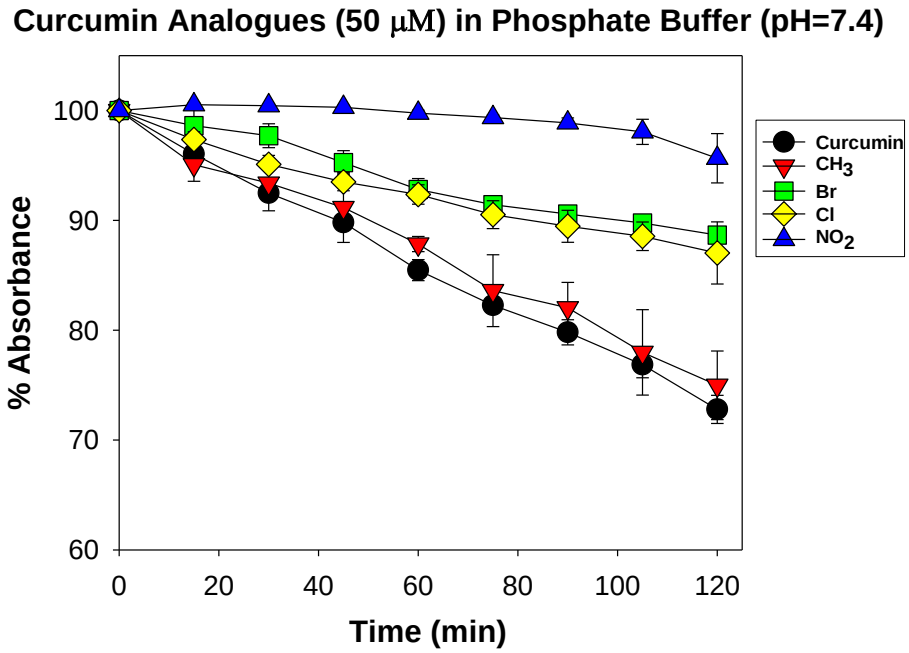

Figure 28. Stability of 7,7'-R-curcumin analyzed with colorimetry assay

2.4 Conclusion

Here in this research, we conducted a SAR study to demonstrate the role of the curcumin structure in its stability in physiological environment. By analyzing stability of different curcumin analogues, we demonstrated that not only the -OH group but also the methoxy group

significantly contribute to curcumin stability. These results also support the proposed mechanism that curcumin degrades at physiological pH by forming phenolic radicals. With this understanding, we can conduct biological studies in vitro and in vivo to study the differences of these curcumin analogues. It is also of great interest to develop an approach to stabilize curcumin so that we can develop applicable curcumin-based therapeutics to exert its anti-cancer effects.

APPENDICES

APPENDIX A

^{1}H NMR SPECTRUM OF SYNTHESIZED CURCUMIN ANALOGUES

Curcumin

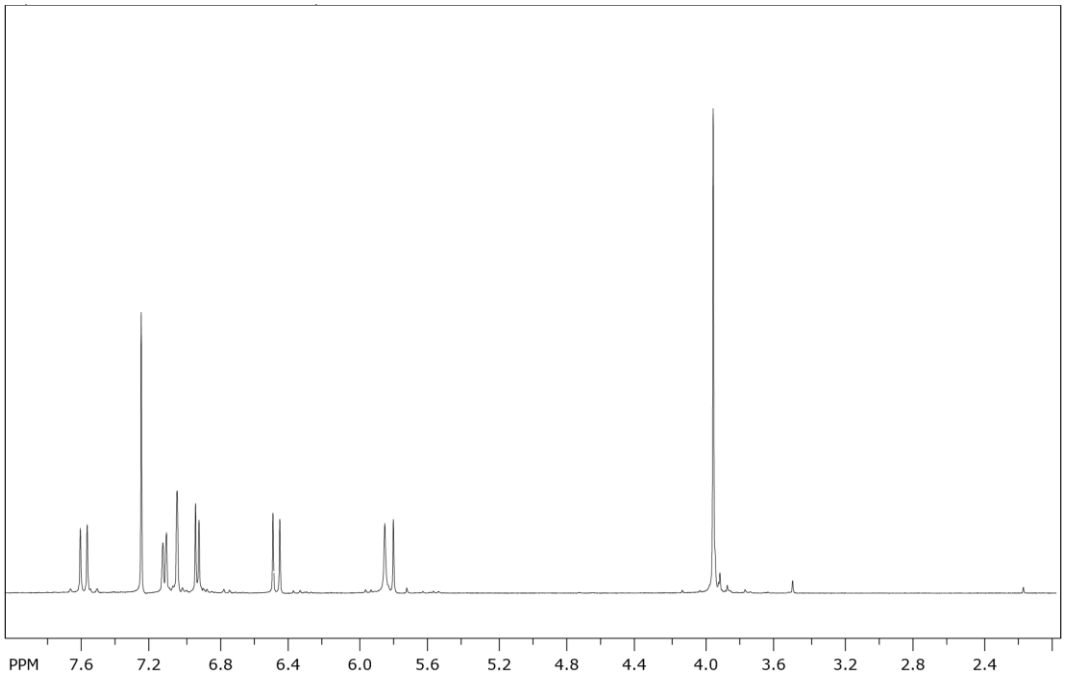

Di-*O*-methyl-curcumin

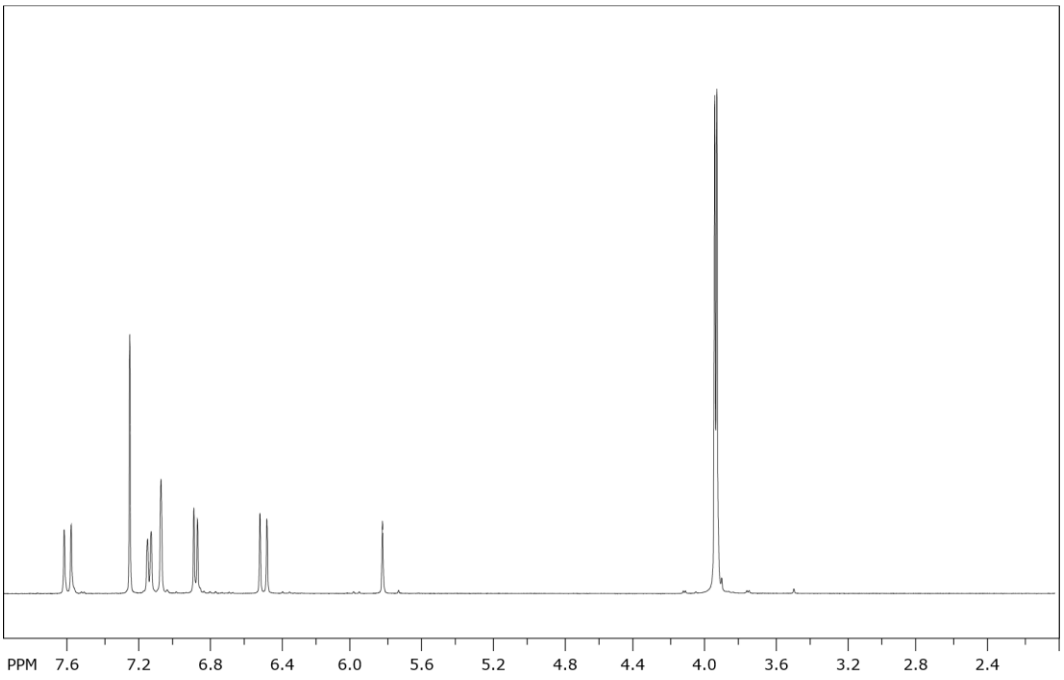

Di-*O*-demethyl-curcumin

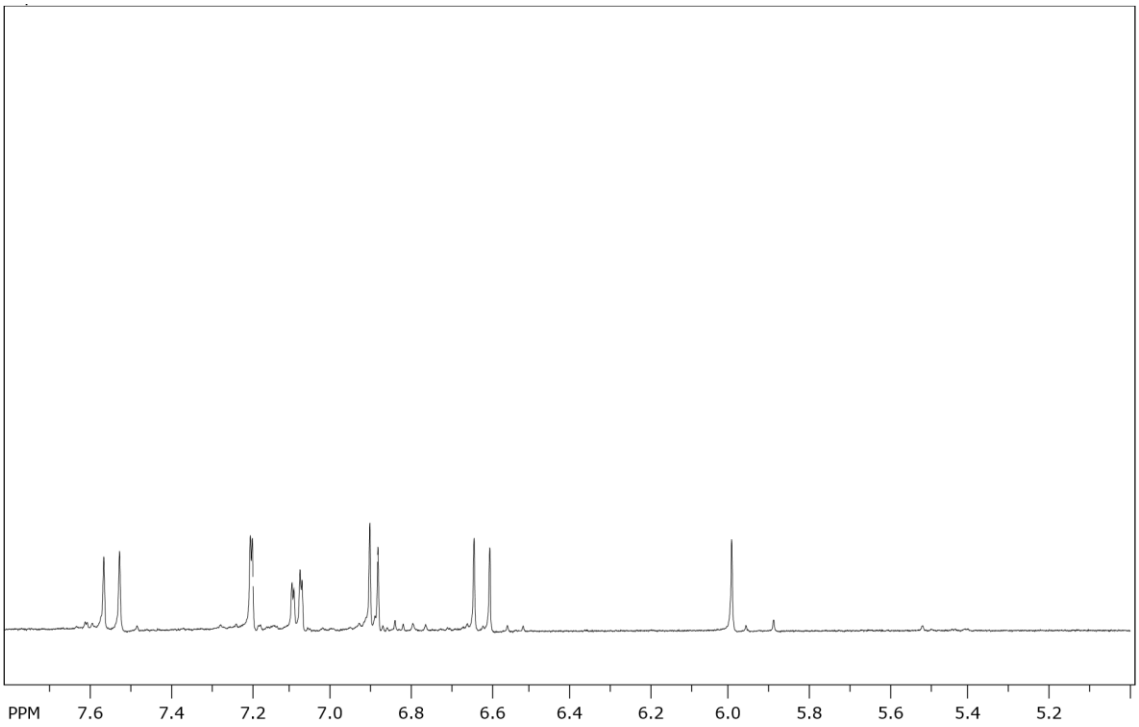

Alkyne-vanillin

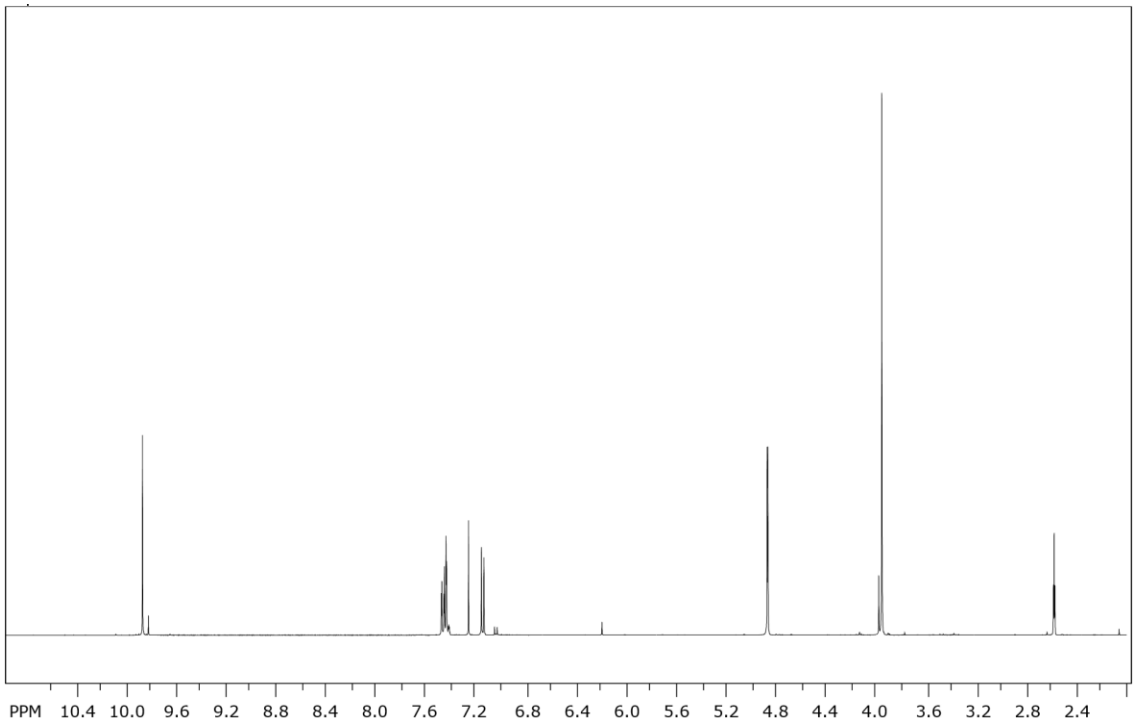

Furoylacetone

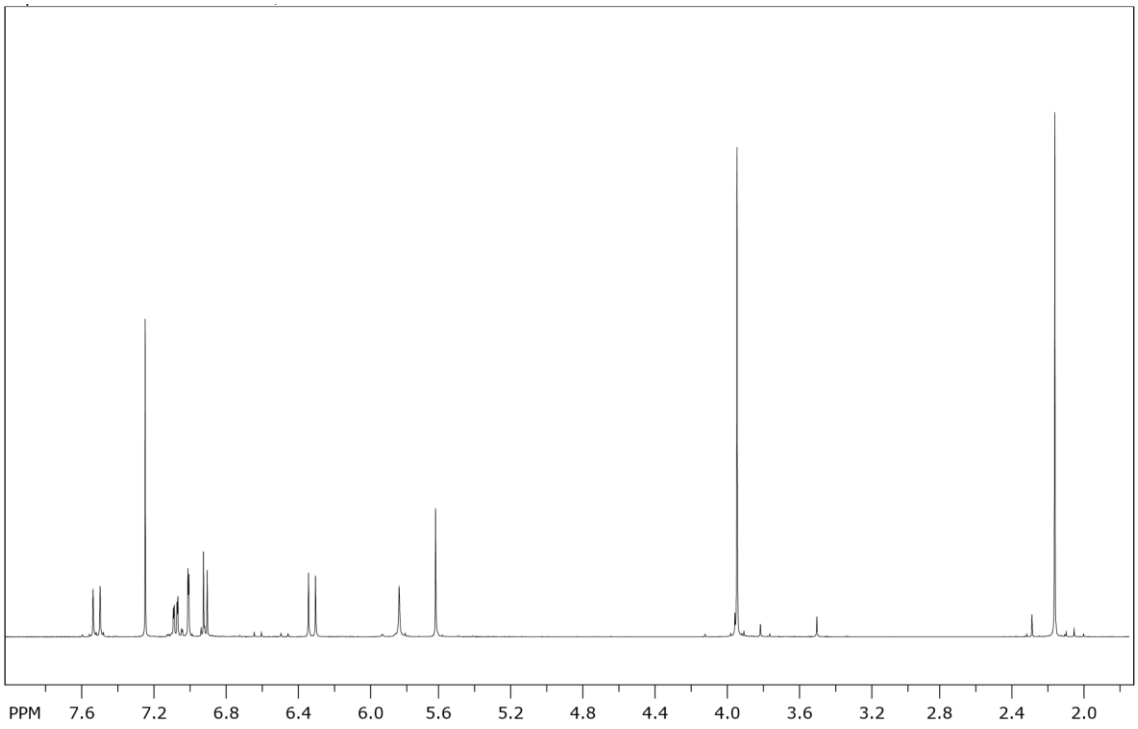

Monoalkyne-curcumin

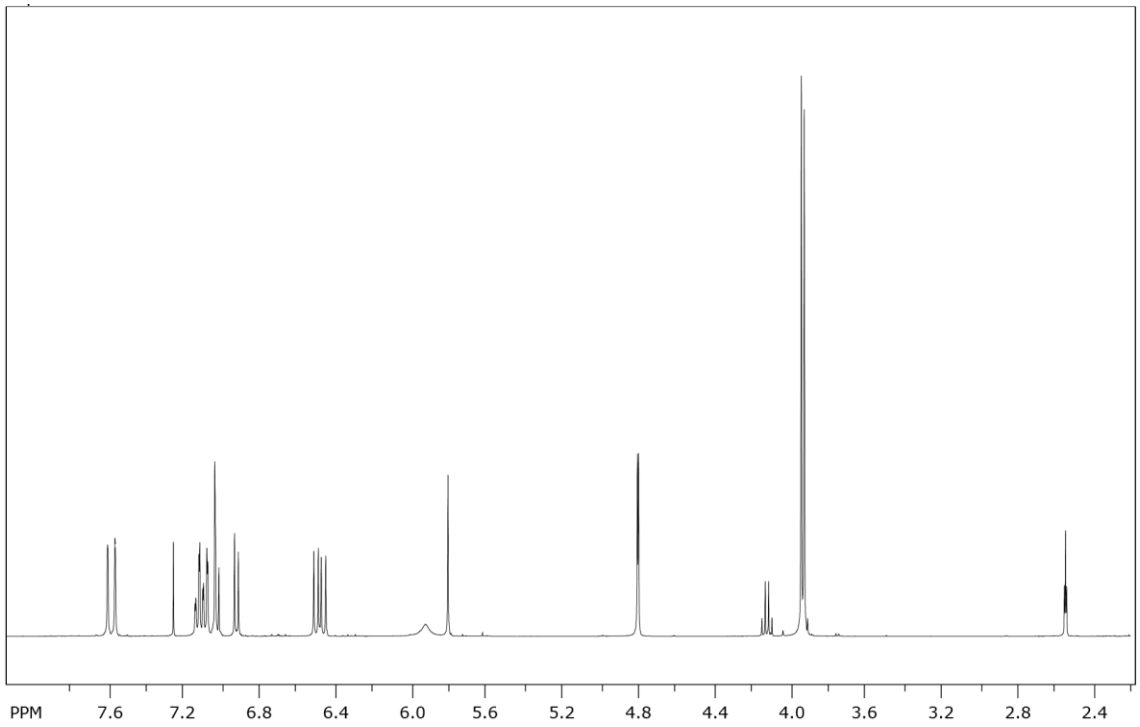

Dialkyne-curcumin

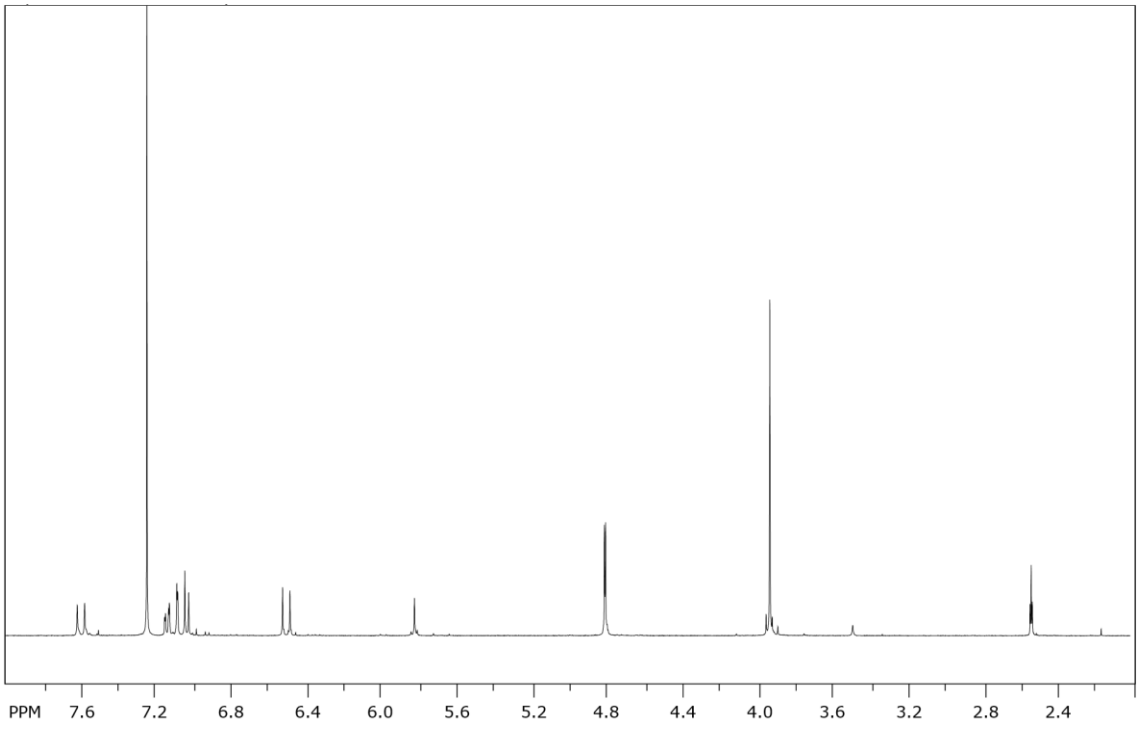

Bisdesmethoxycurcumin

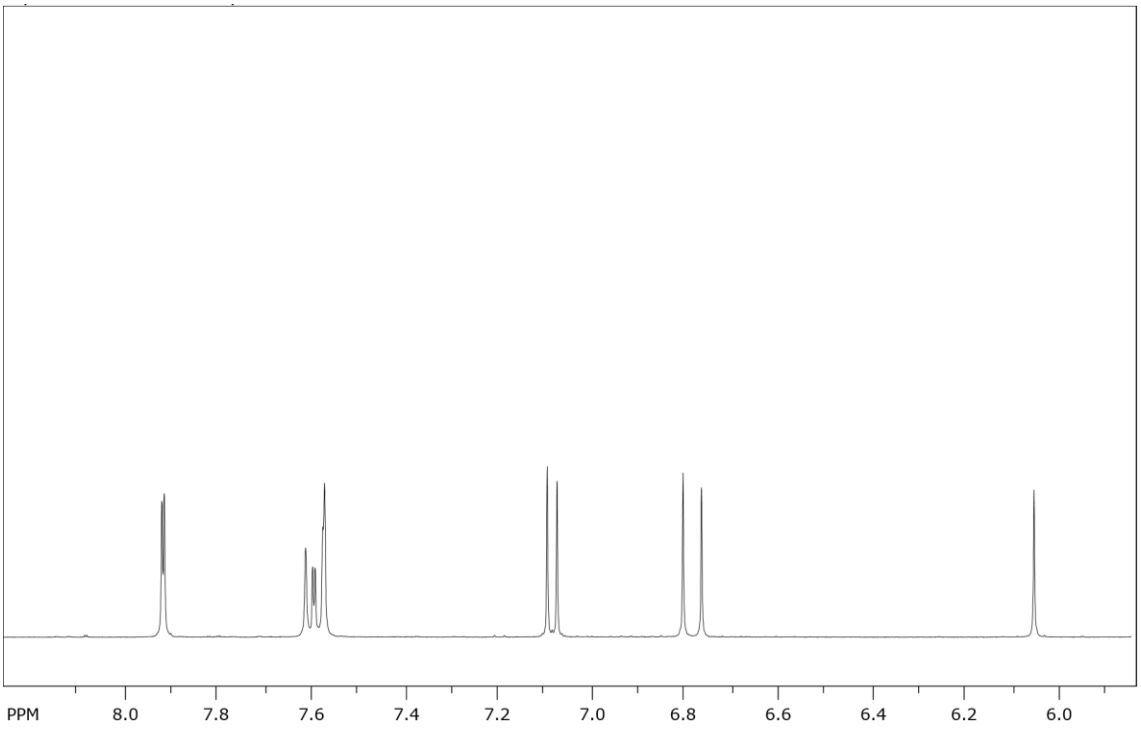

7,7’-methyl-curcumin

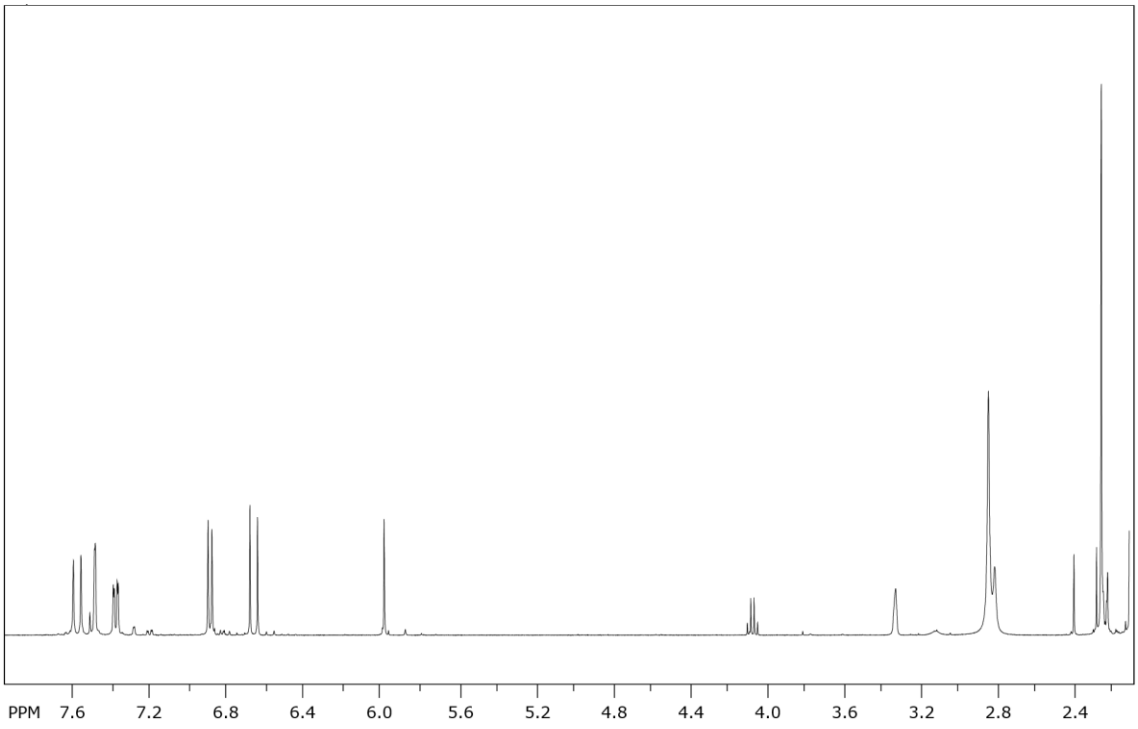

7,7’-nitro-curcumin

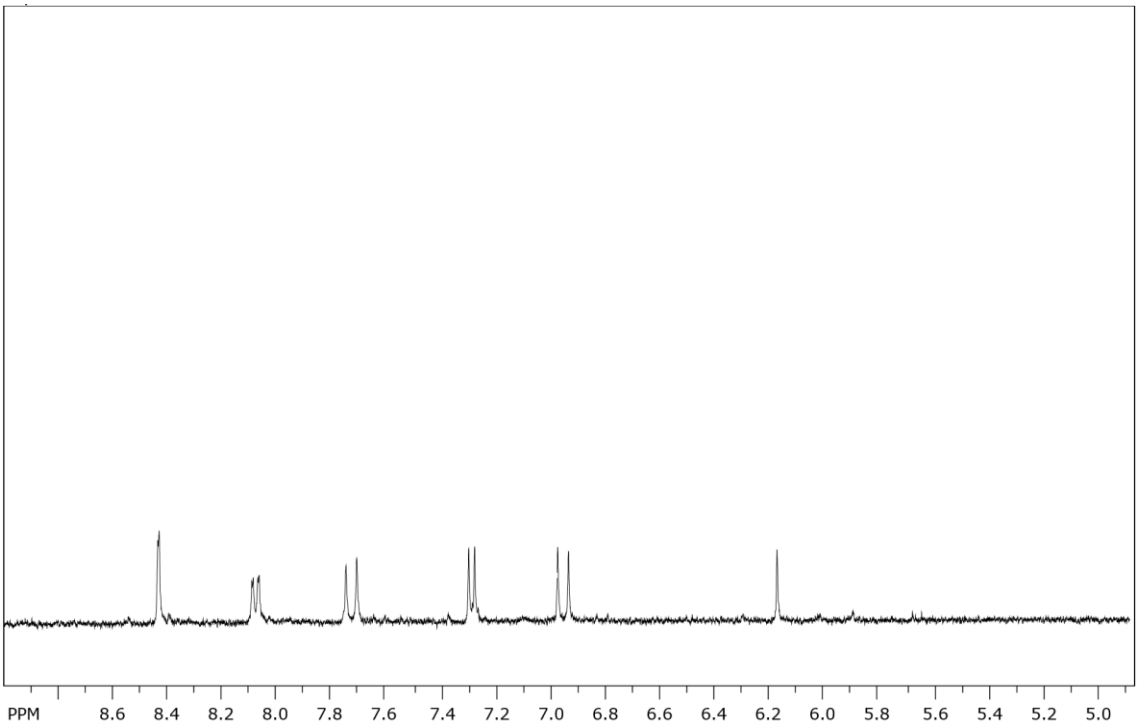

7,7’-bromo-curcumin

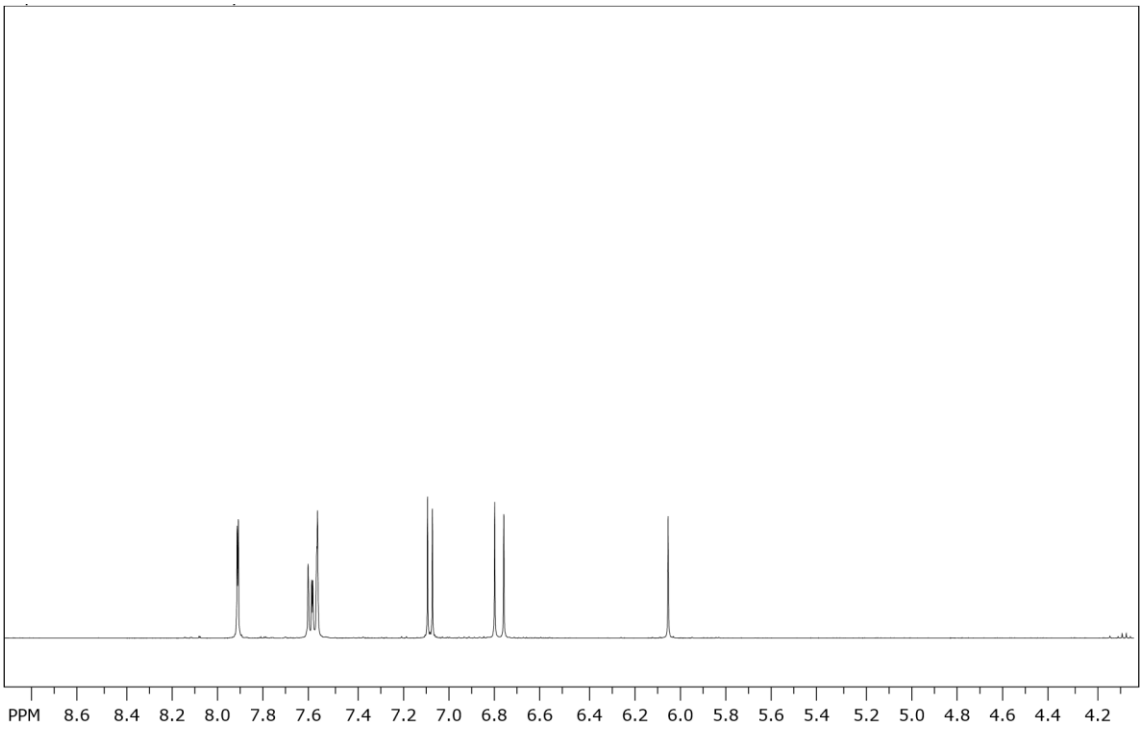

7,7’-chloro-curcumin

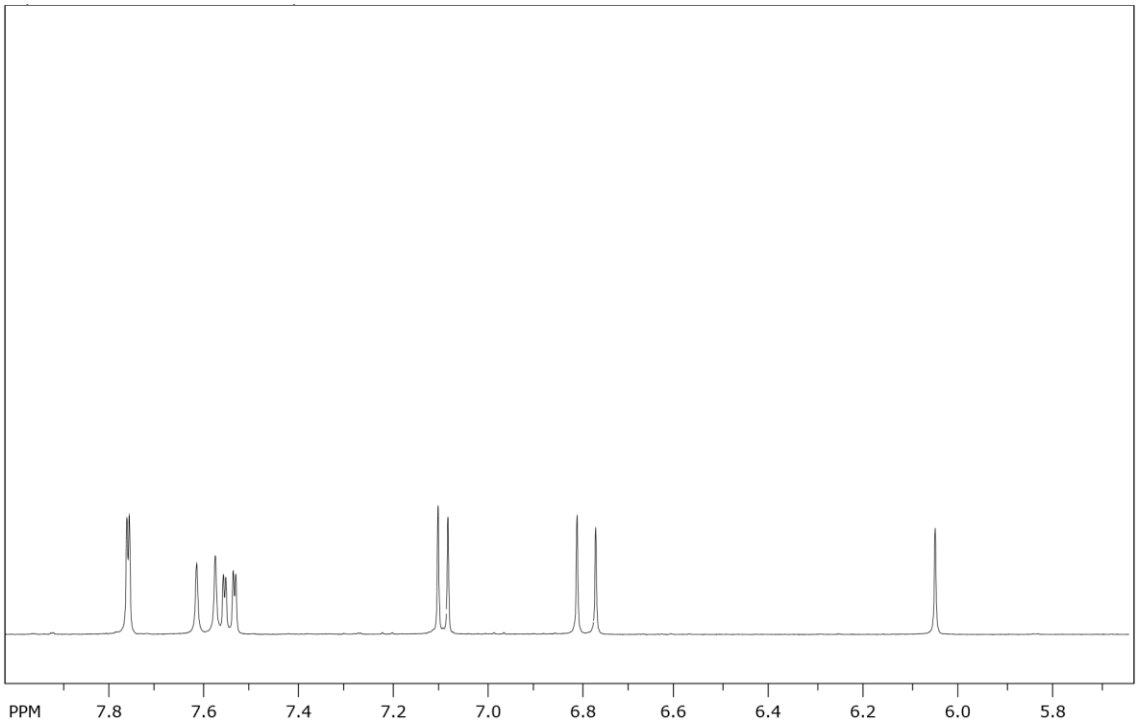

7,7’-fluoro-curcumin

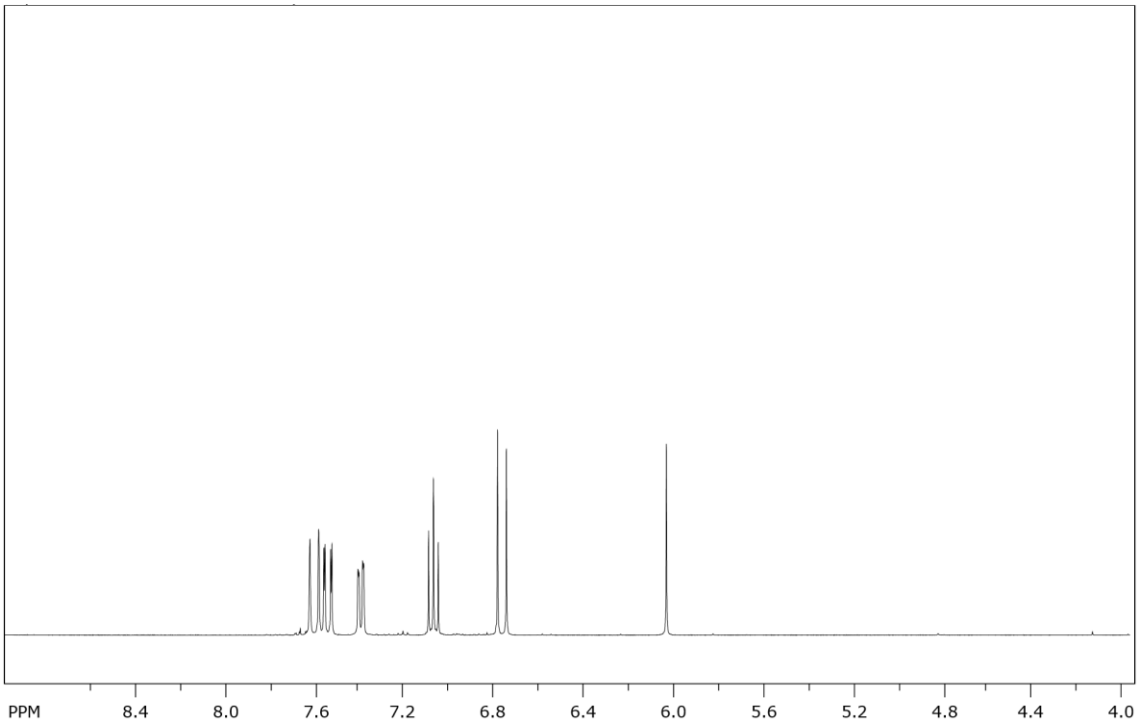

Bicyclopentadione

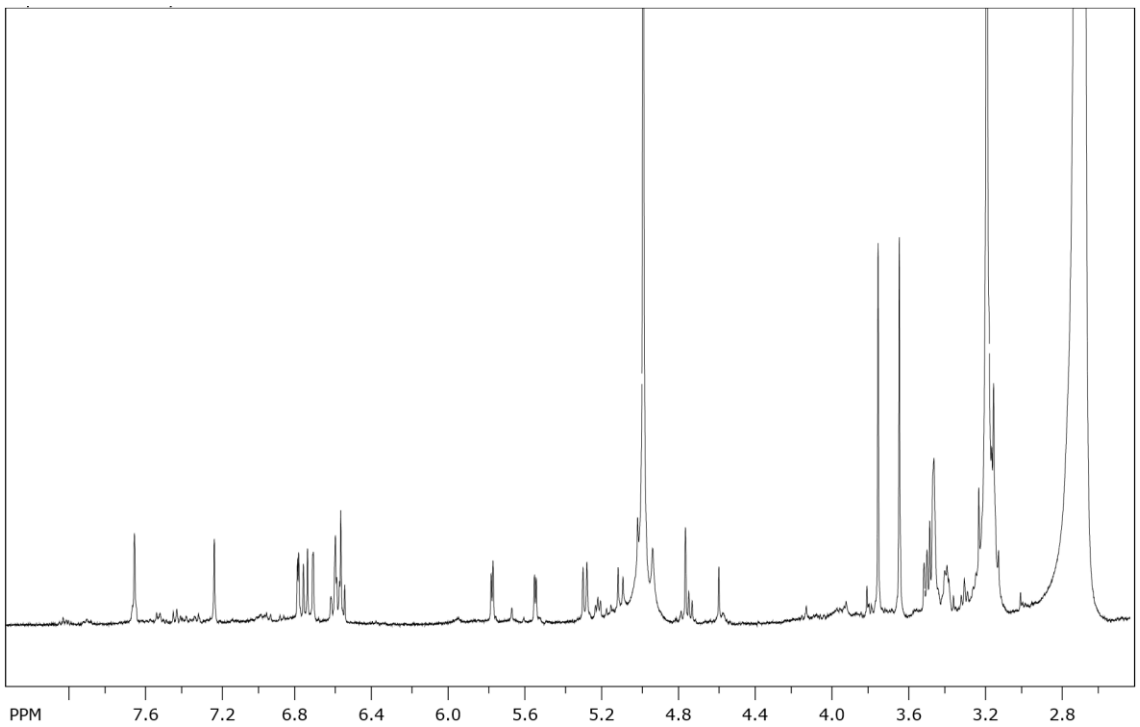

APPENDIX B

HIGH-RESOLUTION MS OF SYNTHESIZED CURCUMIN ANALOGUES

Curcumin

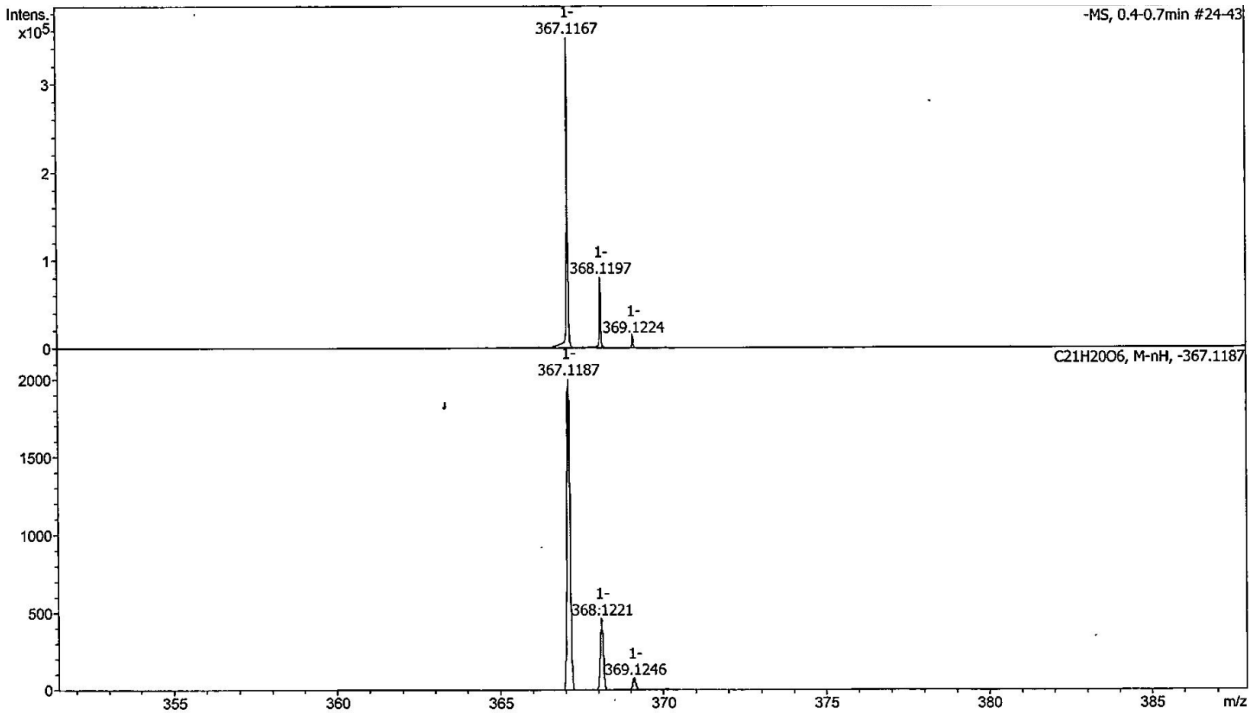

Di-O-methyl-curcumin

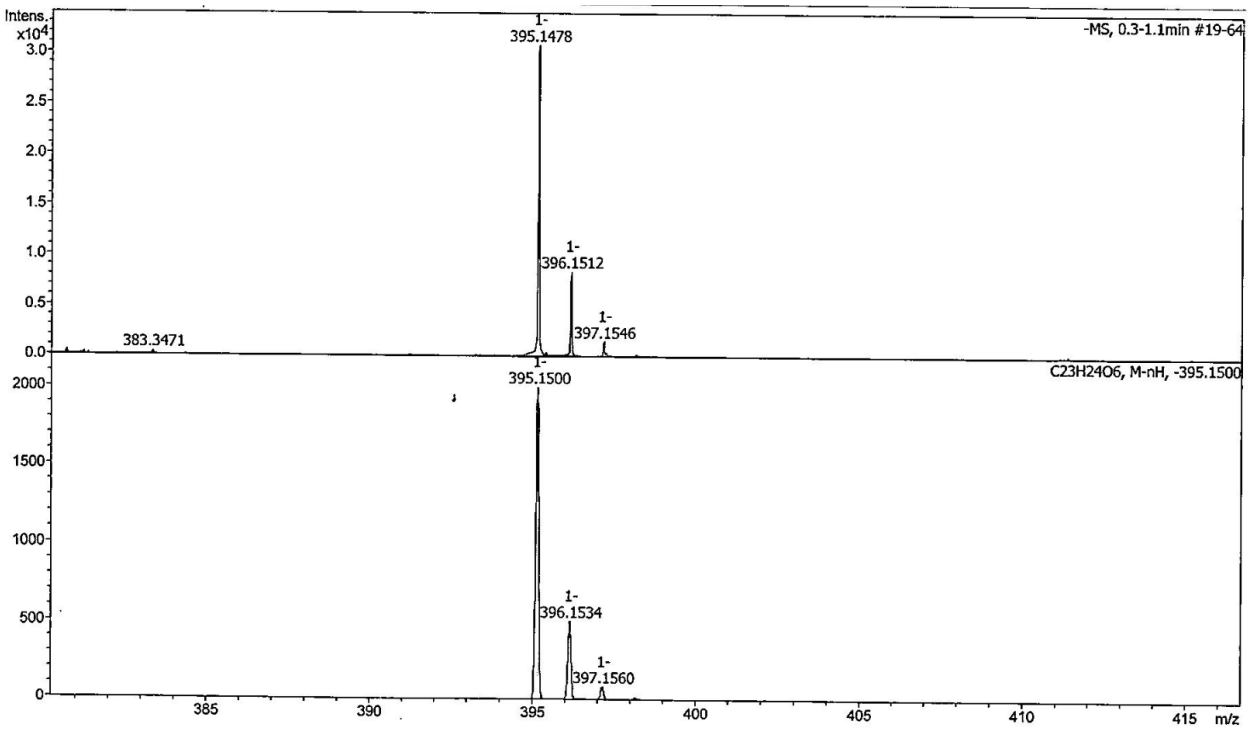

Di-O-demethyl-curcumin

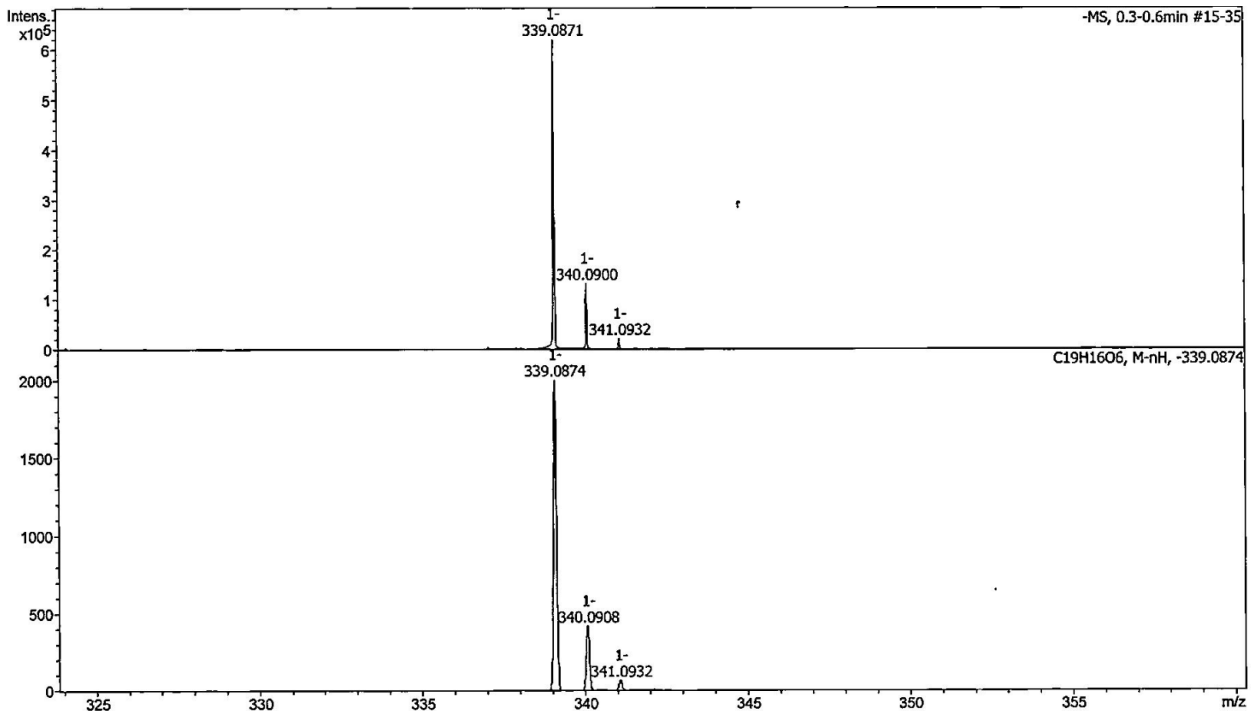

Monoalkyne-curcumin

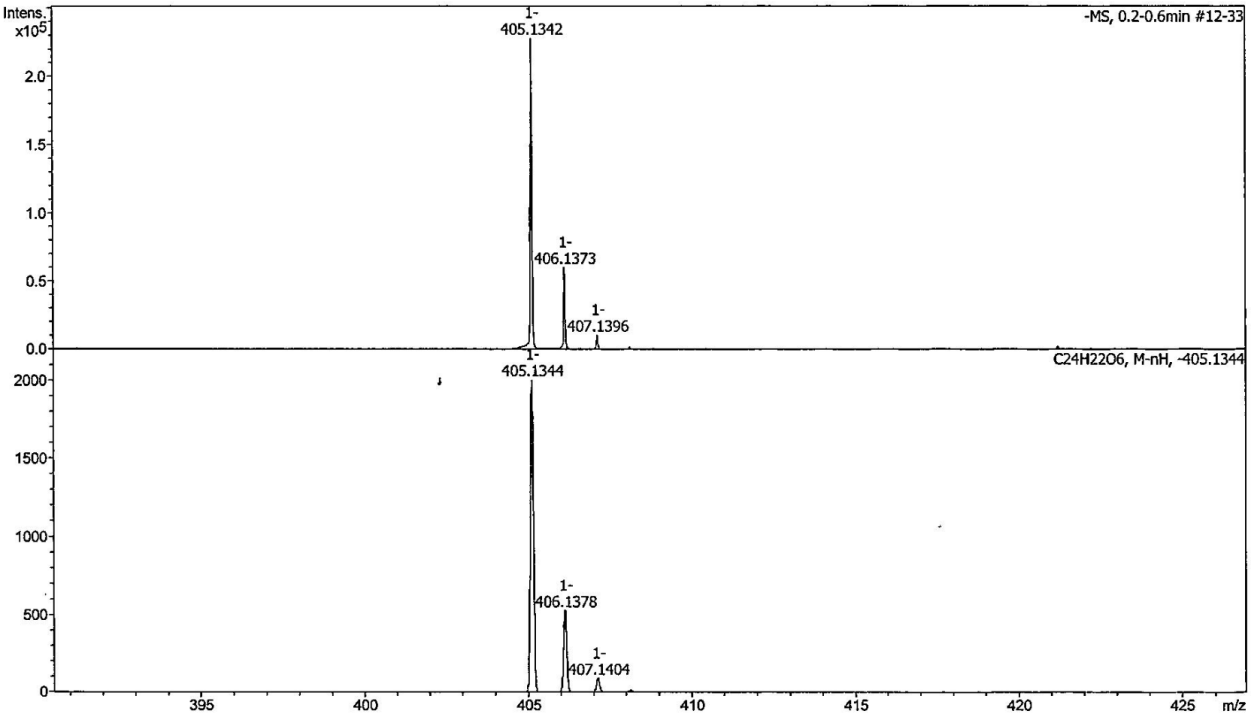

Dialkyne-curcumin

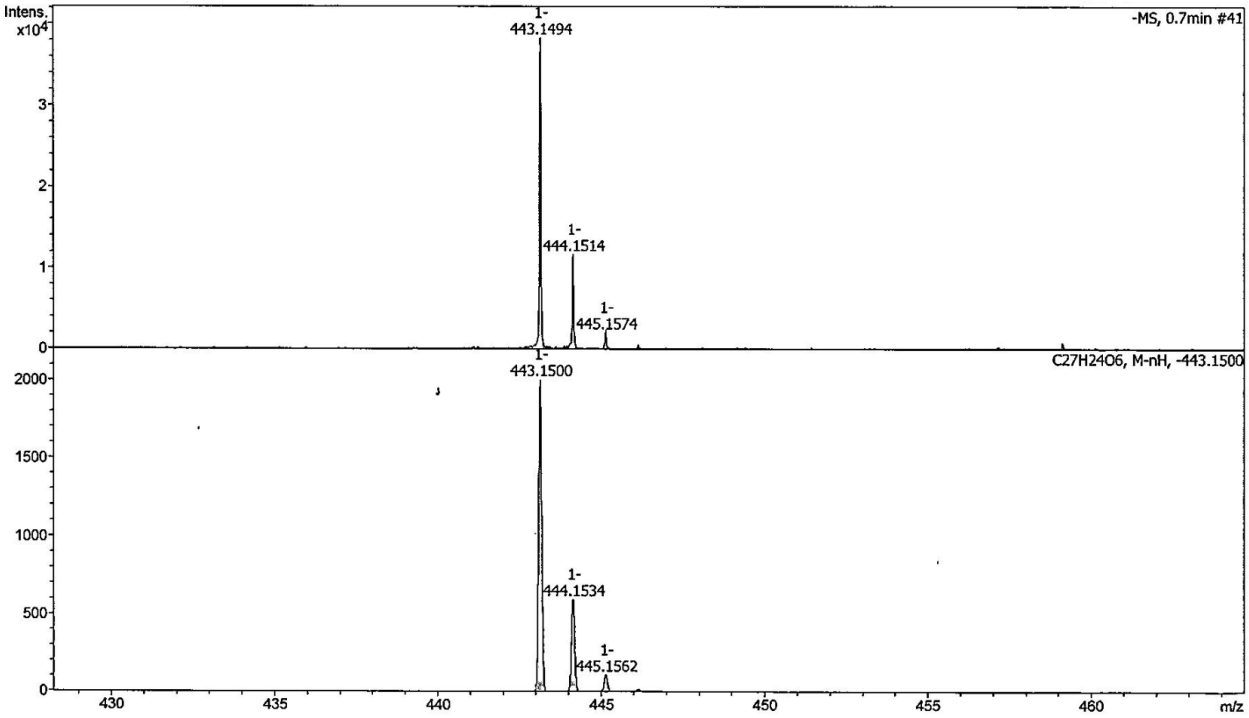

Bisdesmethoxycurcumin

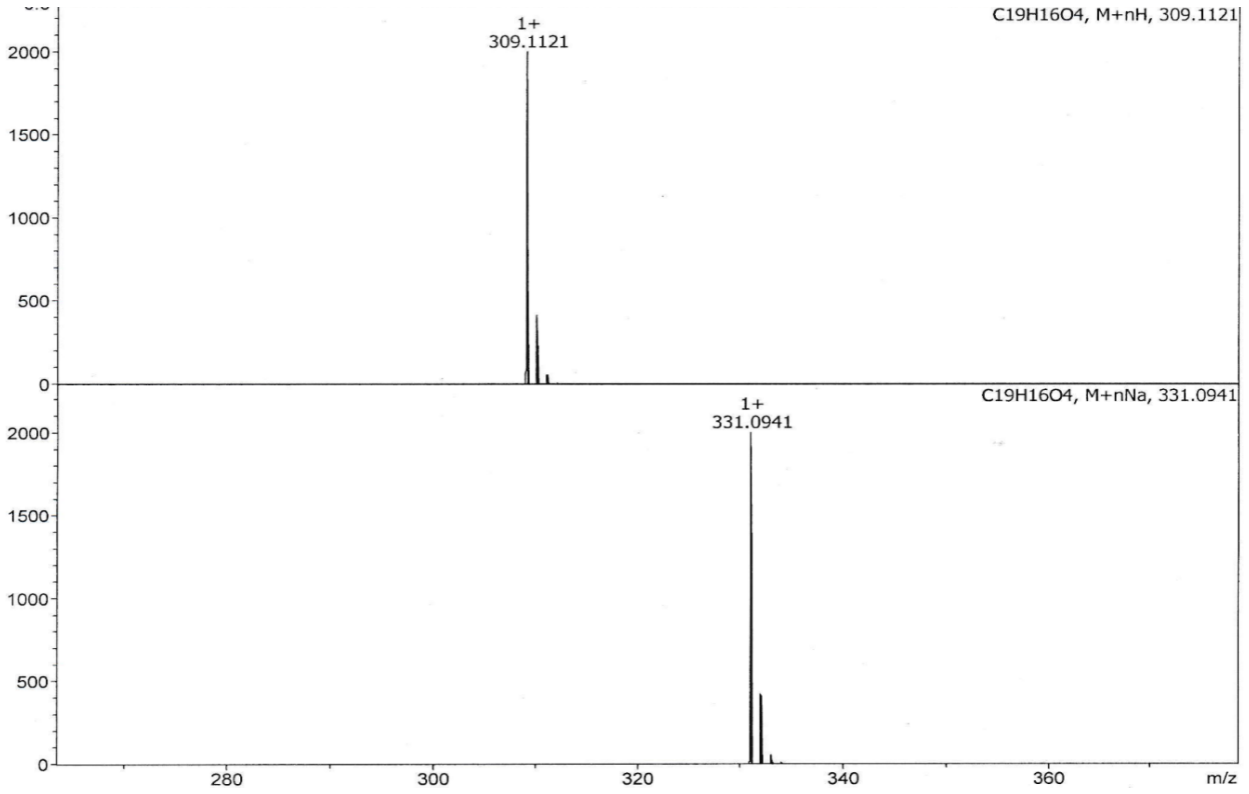

7,7’-methyl-curcumin

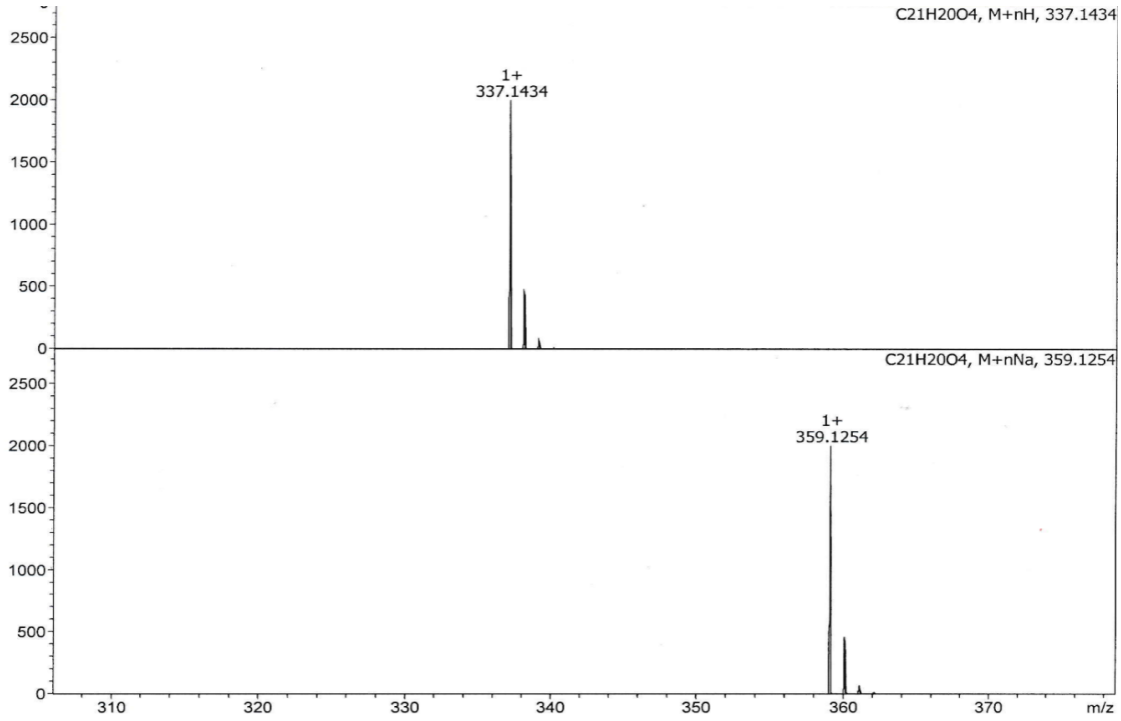

7,7’-nitro-curcumin

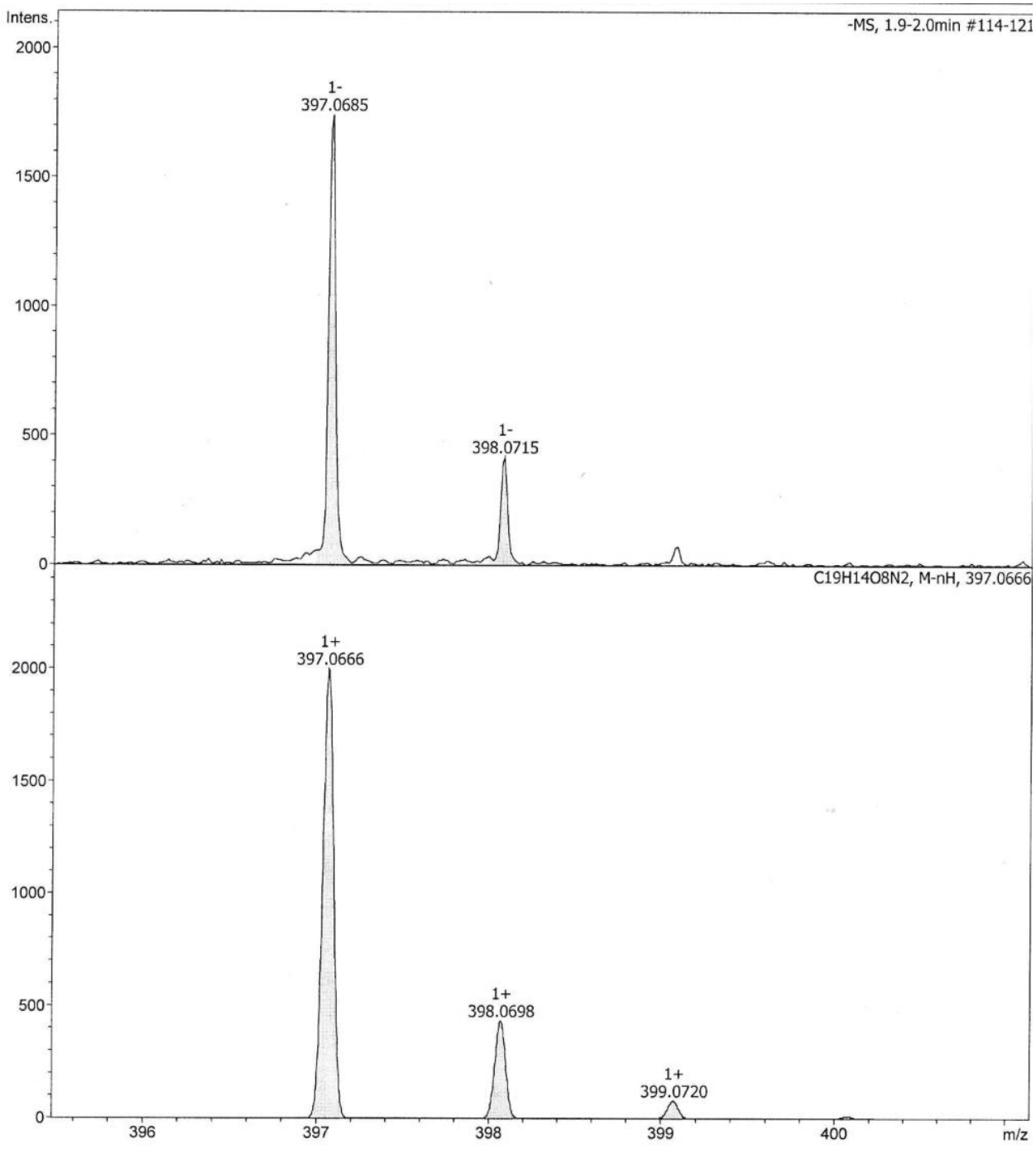

7,7’-bromo-curcumin

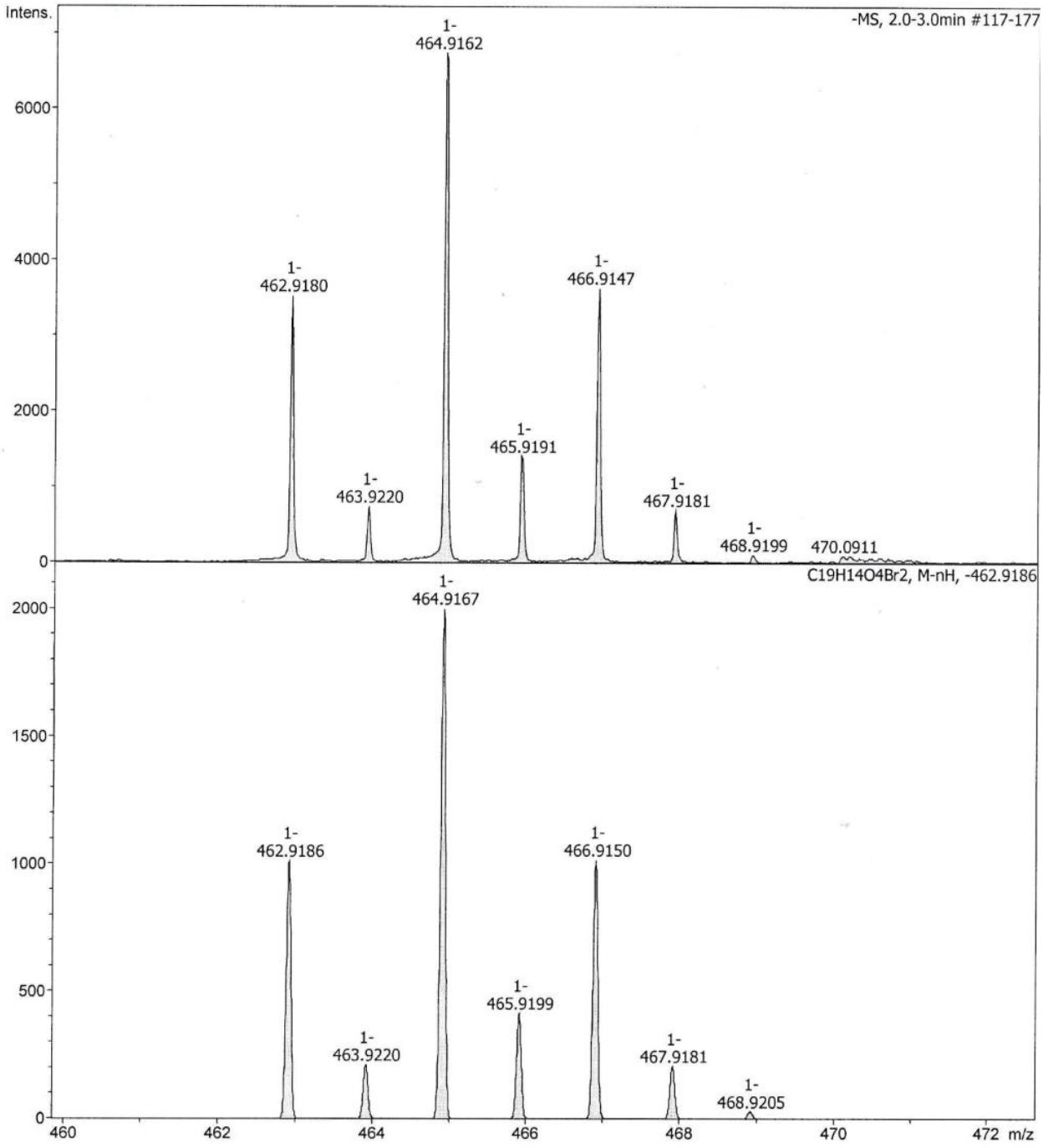

7,7’-chloro-curcumin

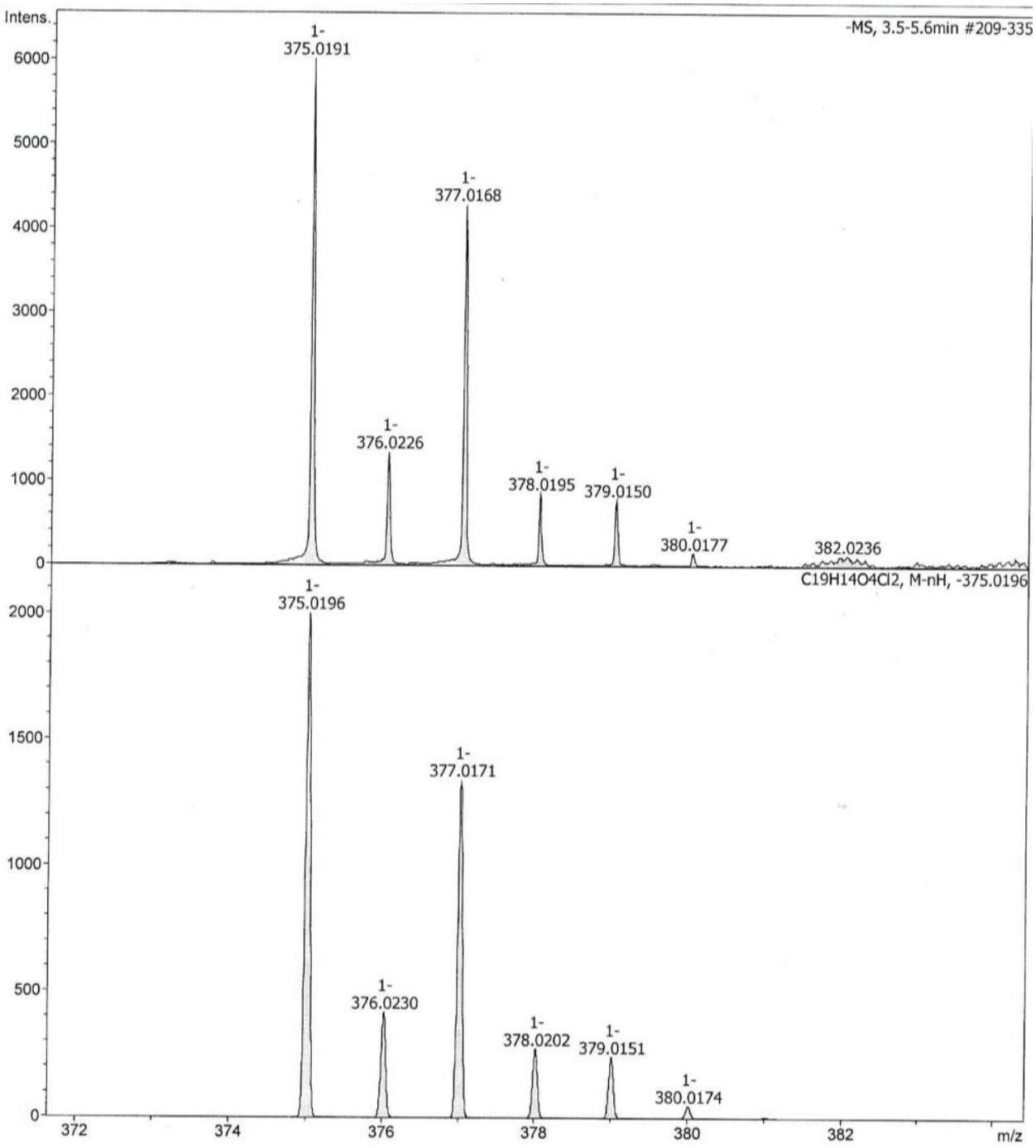

7,7'-fluoro-curcumin

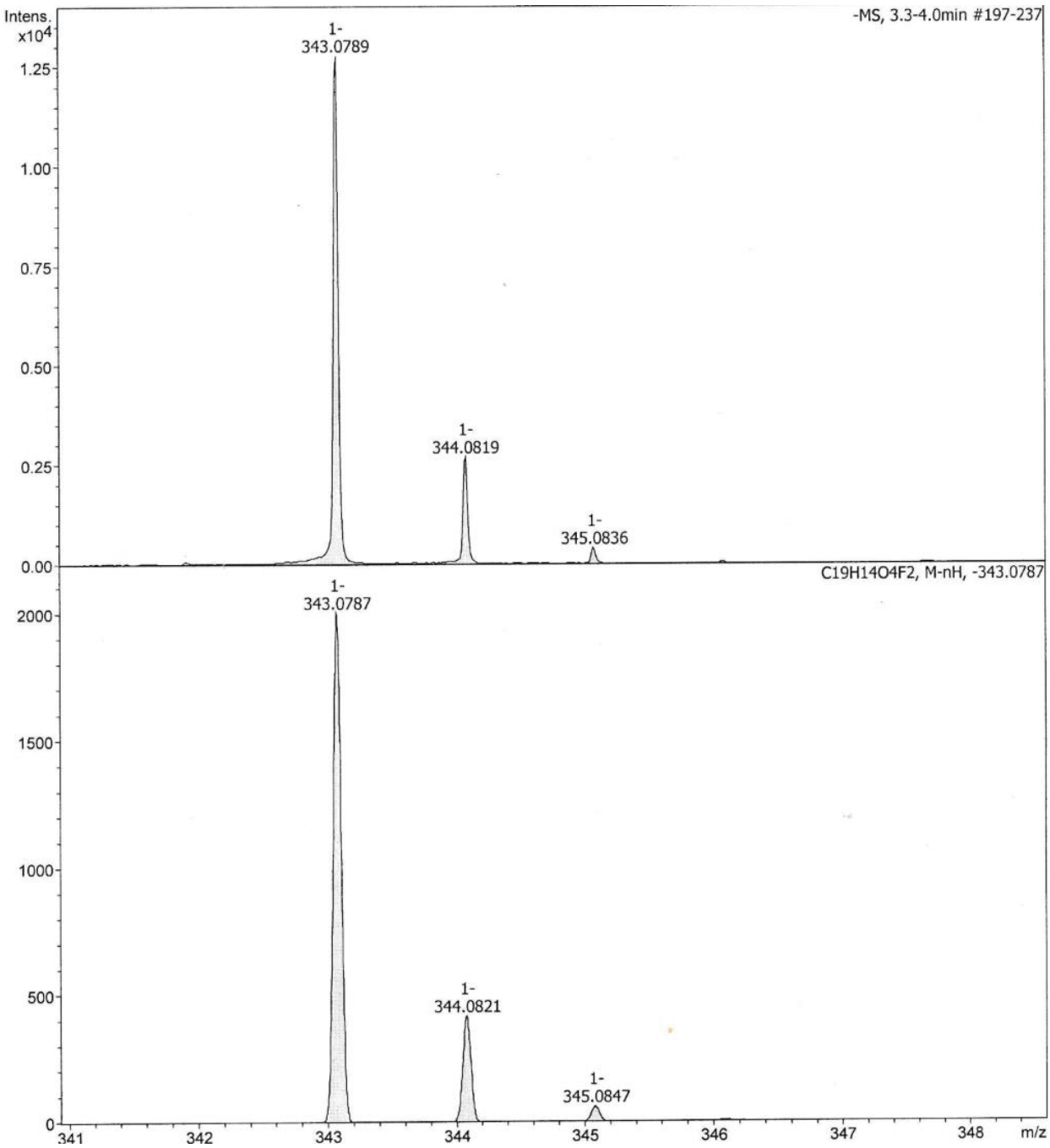

BIBLIOGRAPHY

[1] Goela, A, Kunnumakkarab, A.B., Aggarwalb, B.B., Curcumin as "Curecumin": From kitchen to clinic. *Biochemical Pharmacology*. 2008, 75 (4), 787-809.

[2] Srimal, R.C., Dhawan, B.N., Pharmacology of diferuloyl methane (curcumin), a non-steroidal anti-inflammatory agent. *Journal of Pharmacy and Pharmacology*, 1973, 25 (6), 447–452.

[3] Kuttan, R., Bhanumathy,P., Nirmala, K., George, M.C., Potential anticancer activity of turmeric (Curcuma longa). *Cancer Letter*, 1985, 129 (2), 197–202.

[4] Sharma, O.P., Antioxidant activity of curcumin and related compounds. *Biochemical Pharmacology*, 1976, 25 (15), 1811–1812.

[5] Ruby, A.J., Kuttan, G., Babu, K.D., Rajasekharan, K.N., Kuttan, R., Anti-tumour and antioxidant activity of natural curcuminoids. *Cancer Lett*, 1995, 94, 79–83.

[6] Li, L., Ahmed, B., Mehta, K., Kurzrock, R., Liposomal curcumin with and without oxaliplatin: effects on cell growth, apoptosis, and angiogenesis in colorectal cancer. *Mol Cancer Ther*, 2007, 6, 1276–1282.

[7] Cui, S.X., Qu, X.J., Xie, Y.Y., Zhou, L., Nakata, M., Makuuchi, M., Curcumin inhibits telomerase activity in human cancer cell lines. *Int J Mol Med*, 2006, 18, 227–231.

[8] Aoki, H., Takada, Y., Kondo, S., Sawaya, R., Aggarwal, B.B., Kondo, Y., Evidence that curcumin suppresses the growth of malignant gliomas in vitro and in vivo through induction of autophagy: role of Akt and ERK signaling pathways. *Mol Pharmacol*, 2007, 72 (1), 29–39.

[9] Perry, M.C., Demeule, M., Re ´gina, A., Moumdjian, R., Be ´liveau, R., Curcumin inhibits tumor growth and angiogenesis in glioblastoma xenografts. *Mol Nutr Food Res*, 2010, 54, 1192–1201.

[10] LoTempio, M.M., Veena, M.S., Steele, H.L., Ramamurthy, B., Ramalingam, T.S., Cohen, A.N., Curcumin suppresses growth of head and neck squamous cell carcinoma. *Clin Cancer Res*, 2005, 11, 6994–7002.

[11] Odot, J., Albert, P., Carlier, A., Tarpin, M., Devy, J., Madoulet, C., In vitro and in vivo anti-tumoral effect of curcumin against melanoma cells. *Int J Cancer*, 2004, 111, 381–387.

[12] Beckett, D.M., Pycha, K., Berg, T., Effects of curcumin or tumor growth and muscle mass in a mouse model of cancer cachexia. *Oncology Nursing Forum*, 2008, 35 (3), 455-459.

[13] Lin, Y.G., Kunnumakkara, A.B., Nair, A., Merritt, W.M., Han, L.Y., Armaiz-Pena, G.N., Curcumin inhibits tumor growth and angiogenesis in ovarian carcinoma by targeting the nuclear factor—{kappa}B pathway. *Clin Cancer Res*, 2007, 13, 3423–3430.

[14] Li, L., Braiteh, F.S., Kurzrock R., Liposome-encapsulated curcumin: in vitro and in vivo effects on proliferation, apoptosis, signaling, and angiogenesis. *Cancer*, 2005, 104, 1322–1331.

[15] Kunnumakkara, A.B., Guha, S., Krishnan, S., Diagaradjane, P., Gelovani, J., Aggarwal, B.B., Curcumin potentiates antitumor activity of gemcitabine in an orthotopic model of pancreatic cancer through suppression of proliferation, angiogenesis, and inhibition of nuclear factor-kappaB-regulated gene products. *Cancer Res*, 2007, 67, 3853–3861.

[16] Hong, J.H., Ahn, K.S., Bae, E., Jeon, S.S., Choi, H.Y., The effects of curcumin on the invasiveness of prostate cancer in vitro and in vivo. *Prostate Cancer Prostatic Dis*, 2006, 9, 147–152.

[17] Li, M., Zhang, Z., Hill, D.L., Wang, H., Zhang, R., Curcumin, a dietary component, has anticancer, chemosensitization, and radiosensitization effects by down-regulating the MDM2 oncogene through the PI3K/mTOR/ETS2 pathway. *Cancer Res*, 2007, 67, 1988–1996.

[18] Dorai, T., Cao, Y.C., Dorai, B., Buttyan, R., Katz, A.E., Therapeutic potential of curcumin in human prostate cancer. III. Curcumin inhibits proliferation, induces apoptosis, and inhibits angiogenesis of LNCaP prostate cancer cells in vivo. *Prostate*, 2001, 47, 293–303.

[19] Lev-Aria, S., Starrb, A., Katzburga, S., Berkovicha, L., Rimmona, A., Ben-Yosefa, A., Vexlera, A., Rona. I., Earona, G., Curcumin induces apoptosis and inhibits growth of orthotopic human non-small cell lung cancer xenografts. *Journal of Nutritional Biochemistry* 2014, 25, 843–850.

[20] Huang, M.T., Lou, Y.R., Ma, W., Newmark, H.L., Reuhl, K.R., Conney, A.H., Inhibitory effects of dietary curcumin on forestomach, duodenal, and colon carcinogenesis in mice. *Cancer Res*, 1994, 54, 5841–5847.

[21] Kawamori, T., Lubet, R., Steele, V.E., Kelloff, G.J., Kaskey, R.B., Rao, C.V., Chemopreventive effect of curcumin, a naturally occurring anti-inflammatory agent, during the promotion/progression stages of colon cancer. *Cancer Res*, 1999, 59, 597–601.

[22] Collett, G.P., Robson, C.N., Mathers, J.C., Campbell, F.C., Curcumin modifies Apc(min) apoptosis resistance and inhibits 2-amino 1-methyl-6-phenylimidazo[4,5-b]pyridine (PhIP) induced tumour formation in Apc(min) mice. *Carcinogenesis*, 2001, 22, 821–825.

[23] Shpitz, B., Giladi, N., Sagiv, E., Lev-Ari, S., Liberman, E., Kazanov, D., Celecoxib and curcumin additively inhibit the growth of colorectal cancer in a rat model. *Digestion*, 2006, 74, 140–144.

[24] Ushida, J., Sugie, S., Kawabata, K., Pham, Q.V., Tanaka, T., Fujii, K., Chemopreventive effect of curcumin on N-nitrosomethylbenzylamine-induced esophageal carcinogenesis in rats. *Jpn J Cancer Res*, 2000, 91, 893–898.

[25] Ikezaki, S., Nishikawa, A., Furukawa, F., Kudo, K., Nakamura, H., Tamura, K., Chemopreventive effects of curcumin on glandular stomach carcinogenesis induced by N-methyl-N′-nitro-N-nitrosoguanidine and sodium chloride in rats. *Anticancer Res*, 2001, 21, 3407–3411.

[26] Byun, S.Y., Kim, D.B., Kim, E., Curcumin ameliorates the tumor-enhancing effects of a high-protein diet in an azoxymethane-induced mouse model of colon carcinogenesis. *Nutritional Research,* 2015, 35 (8), 726-735.

[27] Singletary, K., MacDonald, C., Wallig, M., Fisher C., Inhibition of 7,12-dimethylbenz[a]anthracene (DMBA)-induced mammary tumorigenesis and DMBA-DNA adduct formation by curcumin. *Cancer Lett*, 1996, 103, 137–141.

[28] Inano, H., Onoda, M., Inafuku, N., Kubota, M., Kamada, Y., Osawa, T., Chemoprevention by curcumin during the promotion stage of tumorigenesis of mammary gland in rats irradiated with gamma-rays. *Carcinogenesis*, 1999, 20, 1011–1018.

[29] Tanaka, T., Makita, H., Ohnishi, M., Hirose, Y., Wang, A., Mori, H., Satoh, K., Hara, A., Ogawa, H., Chemoprevention of 4-nitroquinoline 1-oxide-induced oral carcinogenesis by dietary curcumin and hesperid comparison with the protective effect of beta-carotene. *Cancer Res*, 1994, 54, 4653–4659.

[30] Azuine, M.A., Bhide, S.V., Adjuvant chemoprevention of experimental cancer: catechin and dietary turmeric in forestomach and oral cancer models. *J Ethnopharmacol*, 1994, 44, 211–217.

[31] Chuang, S.E., Cheng, A.L., Lin, J.K., Kuo, M.L., Inhibition by curcumin of diethylnitrosamine-induced hepatic hyperplasia, inflammation, cellular gene products and cell-cycle-related proteins in rats. *Food Chem Toxicol*, 2000, 38, 991–995.

[32] Huang, A.C., Lin, S.Y., Su, C.C., Lin, S.S., Ho, C.C., Hsia, T.C., Chiu, T.H., Yu, C.S., Ip, S.W., Lin, T.P., Chung, J.G., Effects of curcumin on N-bis(2-Hydroxypropyl) nitrosamine (DHPN)-induced lung and liver tumorigenesis in BALB/c mice *in vivo*. 2008, 22 (6), 781-785.

[33] Pereira, M.A., Grubbs, C.J., Barnes, L.H., Li, H., Olson, G.R., Eto, I., Effects of the phytochemicals, curcumin and quercetin, upon azoxymethane-induced colon cancer and 7,12-dimethylbenz[a]anthracene-induced mammary cancer in rats. *Carcinogenesis*, 1996, 17, 1305–1311.

[34] Hecht, S.S., Kenney, P.M., Wang, M., Trushin, N., Agarwal, S., Rao, A.V., Evaluation of butylated hydroxyanisole, myo-inositol, curcumin, esculetin, resveratrol and lycopene as inhibitors of benzo[a]pyrene plus 4-(methylnitrosamino)-1-(3-pyridyl)-1-butanone-induced lung tumorigenesis in A/J mice. *Cancer Lett*, 1999, 137, 123–130.

[35] Huang, M.T., Lou, Y.R., Xie, J.G., Ma, W., Lu, Y.P., Yen, P., Effect of dietary curcumin and dibenzoylmethane on formation of 7,12-dimethylbenz[a]anthracene-induced mammary tumors and lymphomas/leukemias in Sencar mice. *Carcinogenesis*, 1998, 19, 1697–1700.

[36] Aggarwal, B.B., Shishodia, S., Takada, Y., Banerjee, S., Newman, R.A., Bueso-Ramos, C.E., Curcumin suppresses the paclitaxel-induced nuclear factor-kappaB pathway in breast cancer cells and inhibits lung metastasis of human breast cancer in nude mice. *Clin Cancer Res*, 2005, 11, 7490–7498.

[37] Bachmeier, B., Nerlich, A.G., Iancu, C.M., Cilli, M., Schleicher, E., Vene, R., The chemopreventive polyphenol curcumin prevents hematogenous breast cancer metastases in immunodeficient mice. *Cell Physiol Biochem*, 2007, 19, 137–152.

[38] Farhangia, B., Alizadeh, A.M., Khodayarib, H., Khodayarib, S., Dehghanc, M.J., Khorid, V., Heidarzadehc, A., Khanikie, M., Sadeghiezadehc, M., Najafi F., Protective effects of dendrosomal curcumin on an animal metastatic breast tumor. *European Journal of Pharmacology*, 2015, 758, 188–196.

[39] Ibrahim, A., El-Meligy, A., Fetaih, H., Dessouki, A., Stoica, G., Barhoumi, R., Effect of Curcumin and Meriva on the Lung Metastasis of Murine Mammary Gland Adenocarcinoma. *in vivo*, 2010, 24, 401-408.

[40] Ohashi, Y., Tsuchiya, Y., Koizumi, K., Sakurai, H., Saiki I., Prevention of intrahepatic metastasis by curcumin in an orthotopic implantation model. *Oncology*, 2003, 65, 250–258.

[41] Chen, W.H., Lee, J.Y., Huang, J.Y., Wang, C.C., Chen, W.J., Su, S.F., Huang, C.W., Ho, C.C., Chen, J.J.W., Tsai, M.F., Yu, S.L., Yang, P.C., Curcumin Inhibits Lung Cancer Cell Invasion and Metastasis through the Tumor Suppressor HLJ1. *Cancer Res*, 2008, 68 (18), 7428-7438.

[42] Ichiki, K., Mitani, N., Doki, Y., Hara, H., Misaki, T., Saiki I., Regulation of activator protein-1 activity in the mediastinal lymph node metastasis of lung cancer. *Clin Exp Metastasis*, 2000, 18, 539–545.

[43] Shankar, S., Ganapathy, S., Chen, Q., Srivastava, R.K., Curcumin sensitizes TRAIL-resistant xenografts: molecular mechanisms of apoptosis, metastasis and angiogenesis. *Molecular Cancer*, 2008, 7 (16), 1-13.

[44] Killian, P.H., Kronski, E., Michalik, K.M., Barbieri, O., Astigiano, S., Sommerhoff, C.P., Pfeffer, U., Nerlich, A.G., Bachmeier, B.E., Curcumin inhibits prostate cancer metastasis in vivo by targeting the inflammatory cytokines CXCL1 and -2. Carcinogenesis, 2012, 33 (12), 2507–2519.

[45] Mudduluru, G., George-william, J.N., Muppala, S., Asangani, I.A., Kumarswamy, R., Nelson, L.D., Allgayer, H., Curcumin regulates miR-21 expression and inhibits invasion and metastasis in colorectal cancer. *Biosci Rep*, 2011, 31, 185–197.

[46] Chen, C.C., Sureshbabul, M., Chen, H.W., Lin, Y.S., Lee, J.Y., Hong, Q.S., Yang, Y.C., Yu, S.L., Curcumin Suppresses Metastasis via Sp-1, FAK Inhibition, and E-Cadherin Upregulation in Colorectal Cancer. Evidence-Based Complementary and Alternative Medicine, 2013, 1-17.

[47] Menon, L.G., Kuttan, R., Kuttan, G., Inhibition of lung metastasis in mice induced by B16F10 melanoma cells by polyphenolic compounds. *Cancer Lett*, 1995, 95, 221–225.

[48] Menon, L.G., Kuttan, R., Kuttan, G., Anti-metastatic activity of curcumin and catechin. *Cancer Lett*, 1999, 141, 159–165.

[49] Sharma, R.A., McLelland, H.R., Hill, K.A., Ireson, C.R., Euden, S.A., Manson, M.M., Pharmacodynamic and pharmacokinetic study of oral Curcuma extract in patients with colorectal cancer. *Clin Cancer Res*, 2001, 7, 1894–1900.

[50] Sharma, R.A., Euden, S.A., Platton, S.L., Cooke, D.N., Shafayat, A., Hewitt, H.R., Phase I clinical trial of oral curcumin: biomarkers of systemic activity and compliance. *Clin Cancer Res*, 2004, 10, 6847–6854.

[51] Garcea, G., Jones, D.J., Singh, R., Dennison, A.R., Farmer, P.B., Sharma, R.A., Detection of curcumin and its metabolites in hepatic tissue and portal blood of patients following oral administration. *Br J Cancer*, 2004, 90, 1011–1015.

[52] Carroll, R.E., Benya, R.V., Turgeon, D.K., Vareed, S., Neuman, M., Rodriguez, L., Kakarala, M., Carpenter, P.M., McLaren, C., Meyskens, F.L., Brenner, D.E., Phase IIa clinical trial of curcumin for the prevention of colorectal neoplasia. *Cancer Prevention Research*, 2011, 4 (3), 354-364.

[53] Dhillon, N., Aggarwal, B.B., Li, L., Chiao, P., Sarkar, F., Wolff, R.A., Phase II trial of curcumin (diferuloyl methane), an NF-κB inhibitor, in patients with advanced pancreatic cancer. *J Clin Oncol*,2006, 24, 14151.

[54] Kanai, M., Yoshimura, K., Asada, M., Imaizumi, A., Suzuki, C., Matsumoto, S., Nishimura, T., Mori, Y., Masui, T., Kawaguchi, Y., Yanagihara, K., Yazumi, S., Chiba, T., Guha, S., Aggarwal, B.B., A phase I/II study of gemcitabine-based chemotherapy plus curcumin for patients with gemcitabine-resistant pancreatic cancer. *Cancer Chemotherapy and Pharmacology*, 2011, 68 (1), 157-164.

[55] Mahammedi, H., Planchat, E., Pouget, M., Durando, X., Cure, H., Guy, L., Van-Praagh, I., Savareux, L., Atger, M., Bayet-Robert, M., Gadea, E., Abrial, C., Thivat, E., Chollet, P., Eymard, J.C., The New Combination Docetaxel, Prednisone and Curcumin in Patients with Castration-Resistant Prostate Cancer: A Pilot Phase II Study. *Oncology*, 2016, 90 (2), 69-78.

[56] Bayet-Robert, M., Kwiatkowski, F., Leheurteur, M., Gachon, F., Planchat, E., Abrial, C., Mouret-Reynier, M.A., Durando, X., Barthomeuf, C., Chollet, P., Phase I dose escalation trial of docetaxel plus curcumin in patients with advanced and metastatic breast cancer. *Cancer Biology & Therapy*, 2010, 9 (1): 8-14.

[57] Ravindranath, V., Chandrasekhara N., Absorption and tissue distribution of curcumin in rats. *Toxicology*, 1980, 16, 259–265.

[58] Holder, G.M., Plummer, J.L., Ryan A.J., The metabolism and excretion of curcumin (1,7-bis-(4-hydroxy-3-methoxyphenyl)-1,6-heptadiene-3,5-dione) in the rat. *Xenobiotica*, 1978, 8, 761–768.

[59] Ravindranath, V., Chandrasekhara, N., Absorption and tissue distribution of curcumin in rats. *Toxicology*, 1980, 16, 259–265.

[60] Nimiya, Y., Wang, W., Du, Z., Sukamtoh, E., Zhu, J., Decker, E., Zhang, G., Redox modulation of curcumin stability: Redox active antioxidants increase chemical stability of curcumin. *Molecular Nutrition & Food Research*, 2016, 60 (3), 487-494.

[61] Griesser, M., Pistis, V., Suzuki, T., Tejera, N., Pratt, D.A., Schneider, C., Autoxidative and Cyclooxygenase-2 catalyzed transformation of the dietary chemopreventive agent curcumin. *Journal of Biological Chemistry*, 2011, 286 (2), 1114-1124.